



# Low Earth Orbit Thermal Control Coatings Exposure Flight Tests: A Comparison of U.S. and Russian Results

---

*A. C. Tribble, R. Lukins, and E. Watts  
Rockwell International  
Space Systems Division • Downey, California*

*S. F. Naumov, and V. K. Sergeev  
NPO Energia  
Kaliningrad • Moscow, Russia*

This publication is available from the following sources:

NASA Center for Aerospace Information  
800 Elkridge Landing Road  
Linthicum Heights, MD 21090-2934  
(301) 621-0390

National Technical Information Service (NTIS)  
5285 Port Royal Road  
Springfield, VA 22161-2171  
(703) 487-4650

## CONTENTS

Section		Page
	List of Tables	iv
	List of Figures	v
	Acronyms and Nomenclature	vi
	<b>ABSTRACT</b>	<b>1</b>
<b>1</b>	<b>INTRODUCTION</b>	<b>1</b>
<b>2</b>	<b>SPACE ENVIRONMENT EFFECTS ON MATERIALS - FLIGHT TESTS</b>	<b>1</b>
	2.1 The U.S. Long Duration Exposure Facility (LDEF)	1
	2.2 The Russian Removable Cassette Container (RCC) Experiments	2
<b>3</b>	<b>ORBITAL EXPOSURE CONDITIONS</b>	<b>3</b>
	3.1 Solar Activity and Solar UV Exposure	3
	3.2 Neutral Density and Atomic Oxygen Fluence	7
	3.3 Radiation Environment and Absorbed Dose	8
	3.4 Comparison of LDEF and RCC-1 Environments	11
<b>4</b>	<b>FLIGHT TEST RESULTS</b>	<b>12</b>
	4.1 Summary of RCC-1 Thermal Control Coatings Exposure	12
	4.1.1 Visual Inspection	12
	4.1.2 Surface Morphology	12
	4.1.3 Optical Properties	14
	4.1.3.1 UV/Visible Reflectance Properties	19
	4.1.3.2 Infrared Reflectance	19
	4.1.4 Mass Loss	19
	4.1.5 Chemical Composition Analysis	45
	4.1.6 Conclusions	45
	4.2 Summary of LDEF Thermal Control Coatings Exposure	45
	4.2.1 White Tedlar	47
	4.2.2 A276 White Paint	47
	4.2.3 Z93 White Paint	47
	4.2.4 S13GLO White Paint	48
	4.2.5 YB71 White Paint	52
	4.2.6 Silver Teflon	52
	4.2.7 Chromic Acid Anodized Aluminum	54
	4.2.8 D111 Black	54
	4.2.9 Z302 Black Paint	54
	4.2.10 Z306 Black Paint	54
	4.2.11 Conclusions	55
<b>5</b>	<b>SUMMARY AND CONCLUSIONS</b>	<b>55</b>
	<b>REFERENCES</b>	<b>56</b>

## List of Tables

<b>Table</b>	<b>Title</b>	<b>Page</b>
1	Russian space environment effects on materials flight experiments.	3
2	Russian space environment effects on materials container specifications.	3
3	LDEF environmental exposure conditions.	6
4	Solar activity and atomic oxygen flux during the RCC-1 experiment.	8
5	Russian proton and electron belt fluence predictions for the RCC-1 experiment.	10
6	Radiation dose values for the RCC-1 experiment.	11
7	Comparison of the LDEF and RCC-1 environmental exposure conditions.	12
8	Thermal control coating materials exposed on the RCC-1 experiment.	13
9	Visual inspection of the RCC-1 thermal control coating materials.	14
10	Full scale test results of the RCC-1 thermal control coating materials.	18
11	Post-flight chemical analysis of the RCC-1 thermal control coating materials.	46
12	A partial list of thermal control coating materials on the LDEF.	48
13	Solar absorptance values for LDEF thermal control coating materials - atomic oxygen stimulated outgassing experiment.	49
14	Solar absorptance values for LDEF thermal control coating materials - thermal control surfaces experiment.	48
15	Emittance values for LDEF thermal control coating materials - atomic oxygen stimulated outgassing experiment.	49
16	Emittance values for LDEF thermal control coating materials - thermal control surfaces experiment.	48
17	Post-flight analysis of LDEF thermal control coating samples.	52

## List of Figures

<b>Figure</b>	<b>Title</b>	<b>Page</b>
1	The Long Duration Exposure Facility (LDEF).	2
2	A Recoverable Cassette Container (RCC).	4
3	The Mir Orbital Station (OS).	5
4	Mir OS altitude during the RCC-1 experiment.	5
5	Solar F10.7 vs time.	6
6	Atomic oxygen density as predicted by the MSIS atmospheric model.	7
7	Atomic oxygen density as predicted by the Russian atmospheric model.	9
8	Comparison of U.S. and Russian number density for F10.7 = 100.	9
9	Proton and electron belt fluence predictions for the LDEF and RCC-1 experiments.	10
10	The LDEF mission radiation dose profile.	11
11	Surface morphology of the TP-co-10M coating.	15
12	Surface morphology of the TP-co-12 coating.	16
13	Surface morphology of the TP-co-90 and 40-1-12-88 coatings.	17
14	Diffuse UV/visible reflection spectra of the AK-512-w coating.	20
15	Diffuse UV/visible reflection spectra of the KO-5191 coating.	21
16	Diffuse UV/visible reflection spectra of the KO-5258 coating.	22
17	Diffuse UV/visible reflection spectra of the TP-co-2 coating.	23
18	Diffuse UV/visible reflection spectra of the TP-co-10M coating.	24
19	Diffuse UV/visible reflection spectra of the TP-co-11 coating.	25
20	Diffuse UV/visible reflection spectra of the TP-co-12 coating.	26
21	Diffuse UV/visible reflection spectra of the TP-co-90 coating.	27
22	Diffuse UV/visible reflection spectra of the 40-1-12-88 coating.	28
23	Diffuse UV/visible reflection spectra of the unprotected AK-243 coating.	29
24	Diffuse UV/visible reflection spectra of the unprotected FP-4246 coating.	30
25	Diffuse UV/visible reflection spectra of the quartz covered AK-243 coating.	31
26	Diffuse UV/visible reflection spectra of the quartz covered FP-5246 coating.	32
27	Diffuse UV/visible reflection spectra of the AK-512-g coating.	33
28	Diffuse IR reflection spectra of the AK-512-w coating.	34
29	Diffuse IR reflection spectra of the KO-5191 coating.	35
30	Diffuse IR reflection spectra of the KO-5258 coating.	36
31	Diffuse IR reflection spectra of the TP-co-2 coating.	37
32	Diffuse IR reflection spectra of the TP-co-10M coating.	38

**List of Figures, continued**

<b>Figure</b>	<b>Title</b>	<b>Page</b>
33	Diffuse IR reflection spectra of the TP-co-11 coating.	39
34	Diffuse IR reflection spectra of the TP-co-12 coating.	40
35	Diffuse IR reflection spectra of the TP-co-90 coating.	41
36	Diffuse IR reflection spectra of the AK-243 coating.	42
37	Diffuse IR reflection spectra of the FP-5246 coating.	43
38	Diffuse IR reflection spectra of the AK-512-g coating.	44
39	Solar absorptance vs solar UV exposure for A276 white paint.	50
40	Diffuse reflection spectra for Z93 white thermal control paint.	51
41	Diffuse reflection spectra for YB71 white thermal control paint.	53

**ACRONYMS**

AO	Atomic Oxygen
LDEF	Long Duration Exposure Facility
LEO	Low Earth Orbit
OS	Orbital Station
RCC	Removable Cassette Container
SEE	Space Environment Effects
SEEM	Space Environment Effects on Materials
TCC	Thermal Control Coatings
VAB	Van Allen Belt

**NOMENCLATURE**

n	number density (cm <sup>-3</sup> )
v	velocity (cm/s)
k <sub>a</sub>	angle factor
T	orbital period (s)
<i>subscripts</i>	
AO	atomic oxygen
o	orbital

## **ABSTRACT**

Both the United States (US) and Russia have conducted a variety of space environment effects on materials (SEEM) flight experiments in recent years. A prime US example was the Long Duration Exposure Facility (LDEF), which spent 5 years and 9 months in low Earth orbit (LEO) from April 1984 to January 1990. A key Russian experiment was the Removable Cassette Container experiment, (RCC-1), flown on the Mir Orbital Station from 11 January 1990 to 26 April 1991. This paper evaluates the thermal control coating materials data generated by these two missions by comparing: environmental exposure conditions, functionality and chemistry of thermal control coating materials, and pre- and post-flight analysis of absorptance, emittance, and mass loss due to atomic oxygen erosion. It will be seen that there are noticeable differences in the US and Russian space environment measurements and models, which complicates comparisons of environments. The results of both flight experiments confirm that zinc oxide and zinc oxide orthotitanate white thermal control paints in metasilicate binders, (Z93, YB71, TP-co-2, TP-co-11, and TP-co-12), are the most stable upon exposure to the space environment. It is also seen that Russian flight materials experience broadens to the use of silicone and acrylic resin binders while the US relies more heavily on polyurethane.

## **1 INTRODUCTION**

This paper presents a comparison of US and Russian LEO flight exposure tests on thermal control coatings. The US data was extracted from the LDEF data archive and the Russian data was provided by NPO Energia. The reader is cautioned when using the solar absorptance values to note that in-space and ground based numbers may vary because in-space values may show the effects of oxygen bleaching upon exposure to atomic oxygen (AO). This bleaching may fade during ground tests following re-exposure to oxygen on return to Earth. All semiconductor pigments like ZnO or TiO<sub>2</sub> exhibit substantial bleaching of the reflectance degradation, (from UV exposure in high vacuum), after a few months of re-exposure to air. Except for the in-flight data from LDEF experiment S0069, the results are from specimens exposed to air for several months and bleaching has occurred.

## **2 SPACE ENVIRONMENT EFFECTS ON MATERIALS - FLIGHT TESTS**

### **2.1 The US Long Duration Exposure Facility (LDEF)**

NASA's Long Duration Exposure Facility (LDEF) was a free-flying, 12-sided cylindrical spacecraft, measuring 30 feet, (9.14 m), in length and 14 feet, (4.27 m), in diameter, that was designed to expose a variety of technology experiments to a known LEO environment<sup>1</sup>. The LDEF was three axis stabilized, to ensure highly reliable predictions of environmental exposure conditions, and carried 57 separate experiments in areas such as: materials, coatings, thermal systems, power, propulsion, space science, electronics, and optics. The location of a specific experiment is described by referencing a row (1 - 12) and a column (A - F) as shown in Figure 1. Because the LDEF was three axis stabilized, the location of an experiment on the vehicle played a significant role in

determining its environmental exposure conditions, (atomic oxygen fluence, solar exposure, radiation, ...). Most of the experiments were passive with the majority of the data resulting from post flight analysis.

The LDEF was placed in LEO by the Space Shuttle Challenger in April of 1984, with the intention of remaining in orbit for one full year until capture and retrieval on a later mission. Before the retrieval could occur the Shuttle fleet was grounded as the result of the Challenger accident and it was 5 years and 9 months before the spacecraft was returned in January of 1990 by the Shuttle Columbia. Post-flight analysis of the LDEF generated a wealth of data on the interaction of materials and systems with the LEO environment. These data have been presented at three dedicated post-retrieval symposiums and integrated into the Materials and Processes Technical Information Service (MAPTIS) database<sup>2-6</sup>.

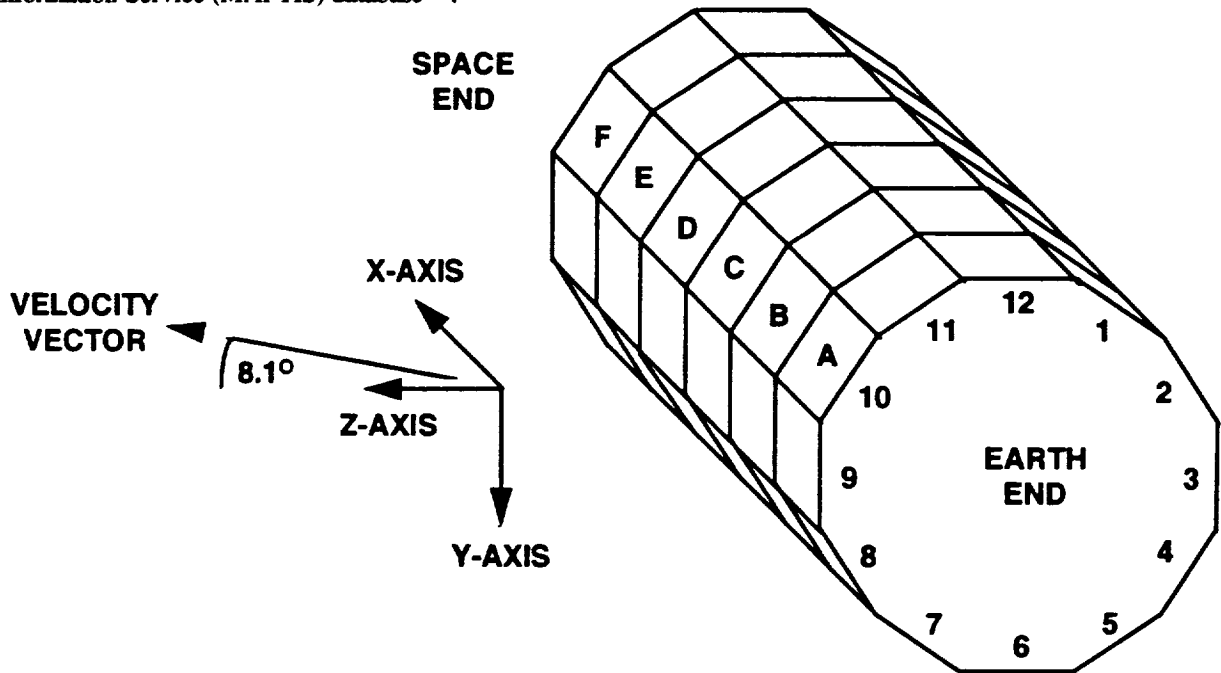


Figure 1. The Long Duration Exposure Facility (LDEF).

Because the LDEF provides the largest and most complete United States (US) space environment effects on materials database, LDEF data will serve as the U.S. benchmark for comparison to similar Russian results.

## 2.2 The Russian Removable Cassette Container (RCC) Experiments

In parallel with the US efforts a number of space environment effects on materials (SEEM) experiments have been conducted by the Russians aboard the Salyut and Mir Orbital Stations (OS). Eight experiments containing about 300 samples of various types of materials and thermal control coatings (TCC's) have been tested in the last ten years, as shown in Table 1. The material samples were exposed to the space environment via removable cassettes which were carried aloft interior to the spacecraft during re-supply missions, placed on the exterior of the station by cosmonauts, retrieved at a later date, and returned to Earth for analysis. Two types of cassettes, the FM-

110 and the removable cassettes container (RCC), have been utilized. The physical differences in the earlier FM-110 and current RCC cassettes are listed in Table 2. A picture of an RCC is provided in Figure 2.

The Russian materials data presented in the remainder of this paper were obtained by the RCC-1 experiment which was delivered to the Mir station on 24 August 1989, exposed to the space environment for 470 days between 11 January 1990 and 26 April 1991, and returned to the ground on 20 May 1991. The RCC-1 was installed on the transfer compartment body of the Mir station, as depicted in Figure 3. The normal to the material samples was perpendicular to the Mir station surface. During the flight the Mir was in LEO with an apogee in the range 380 - 430 km, perigee in the range 360 - 390 km, (for an average altitude of 385 km), and an inclination of 51.6 degrees as shown in Figure 4.

**Table 1. Russian space environment effects on materials flight experiments.**

Station	Cassette	Installation Date	Removal Date	Exposure (days)
Salyut 6	FM-110 No. 11	29 September 77	29 July 78	312
Salyut 7	FM-110 No. 16	19 April 82	30 July 82	99
Salyut 7	FM-110 No. 15	03 November 83	25 July 84	270
Salyut 7	FM-110 No. 17	25 July 84	28 May 86	672
Mir	FM-110 No. 19	16 June 87	26 February 88	255
Mir	FM-110 No. 21	26 February 88	11 January 90	685
Mir	RCC-1	11 January 90	26 April 91	470
Mir	RCC-2	25 January 90	21 February 92	756

**Table 2. Russian space environment effects on materials container specifications.**

	FM-110	RCC
<b>Cassette</b>		
- closed	135 x 90 x 15	210 x 255 x 40
- open	215 x 90 x 10	400 x 255 x 20
<b>Rack</b>		
- length	-	400
- diameter	-	15
- ball end diam.	-	36
<b>Sample</b>		
- dimension	-	30 x 30 x 2
- number	18	70
- mass	0.30 kg	2.0 kg
Dimensions are in mm		

### 3 ORBITAL EXPOSURE CONDITIONS

#### 3.1 Solar Activity and Solar UV Exposure

A standard measure of solar activity is the solar output at 10.7 cm wavelength, commonly known as the F10.7 value. As shown in Figure 5 the LDEF was launched just before solar minimum and remained in orbit until just before solar maximum. Conversely, the RCC-1 experiment took place during solar maximum. Note that while

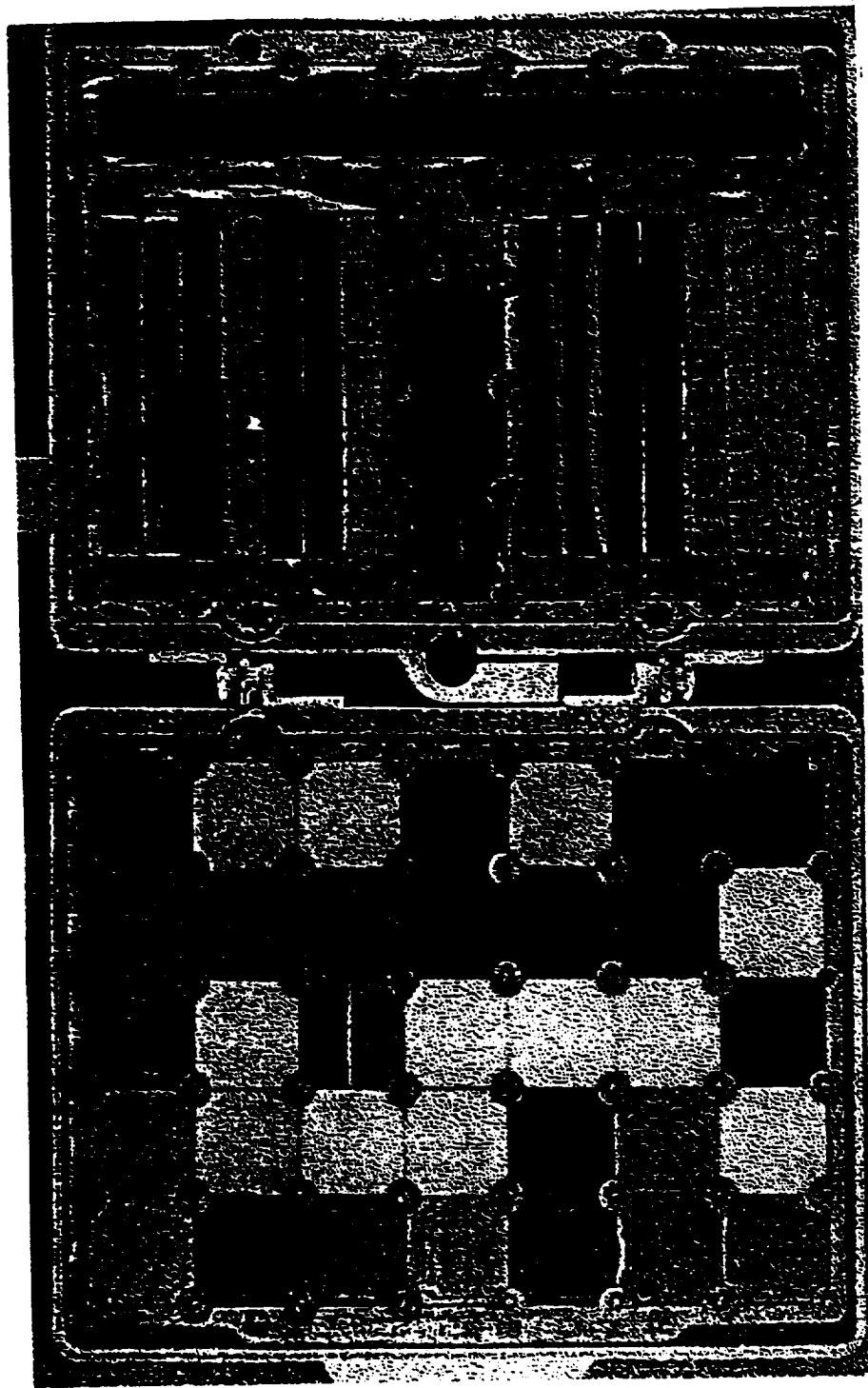


Figure 2. A Removable Cassette Container (RCC).

both US and Russian observations confirm this fact, there is significant disagreement as to the actual F10.7 value. The maximum US value recorded is approximately 200 and the curve exhibits a dual peak, in mid 1989 and late 1992, separated by a local minimum in mid 1990. Two separate Russian values were quoted by NPO Energia, with a maximum value of approximately 280. No further details on the nature of these predictions is available, but neither source indicates the dual peaks noted by the US. The first source records the maximum F10.7 value in early 1991, while the second source records the maximum value in mid 1990. As will be discussed in the next section, the F10.7 value is directly related to neutral atmospheric density. Consequently, the F10.7 disagreement will propagate into a disagreement in neutral density.

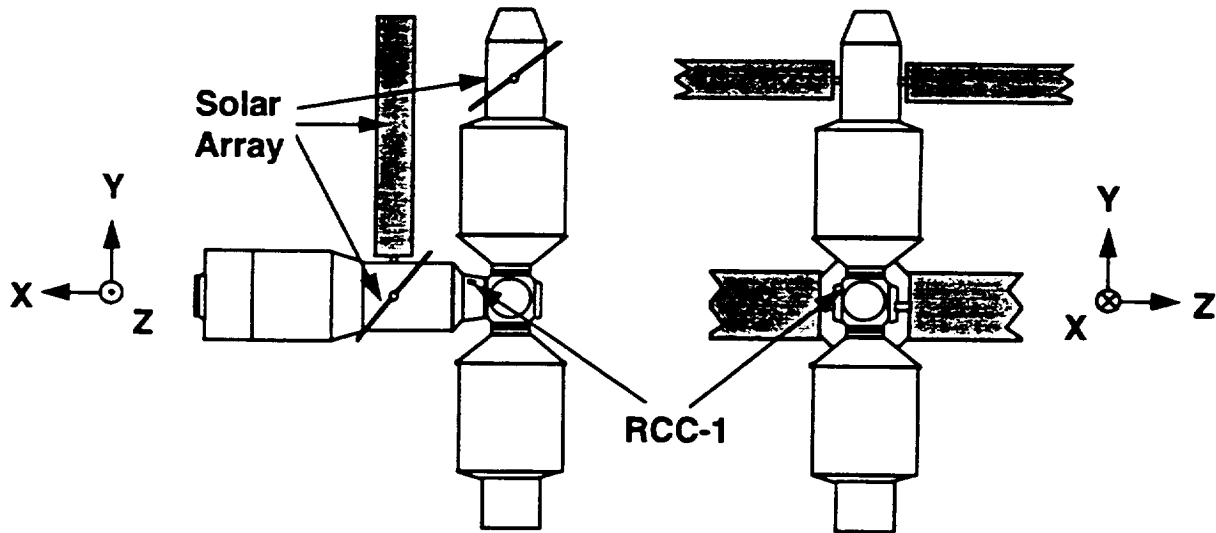


Figure 3. The Mir Orbital Station (OS).

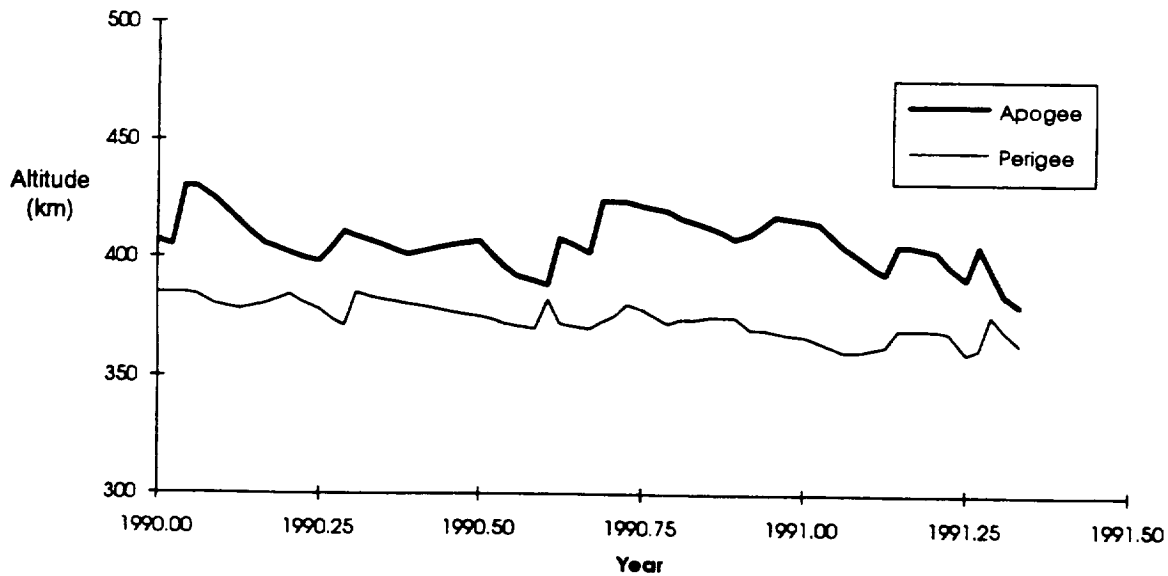


Figure 4. Mir OS altitude during the RCC-1 experiment.

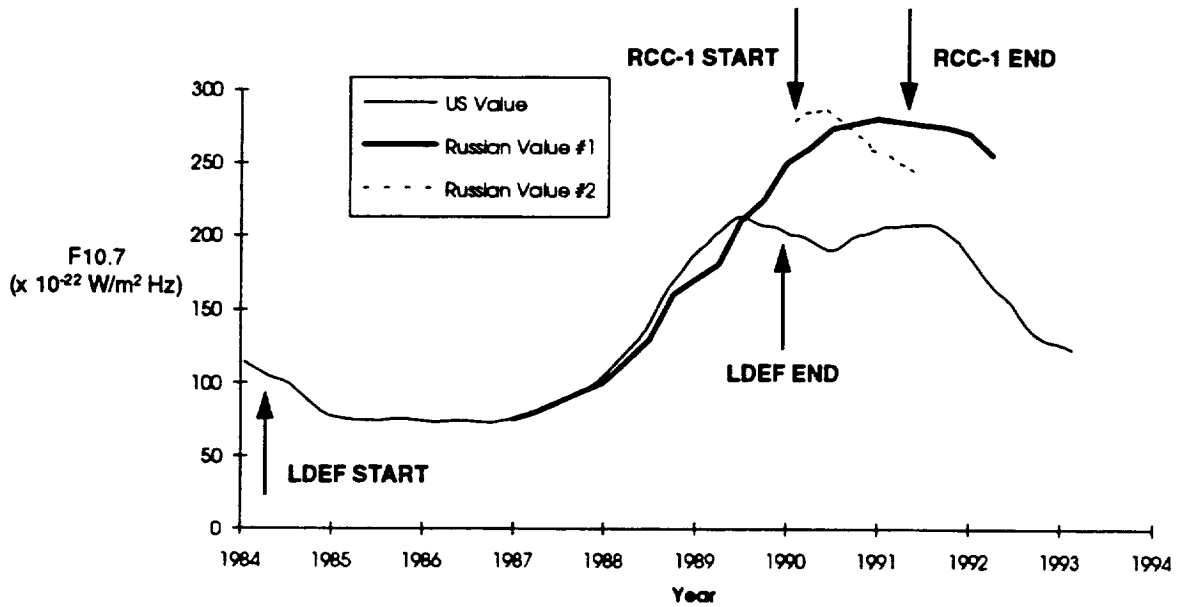


Figure 5. Solar F10.7 vs. time.

The LDEF sun exposure is indicated in Table 3. Because of the duration of the experiment, 5 years and 9 months, the sun exposure for all LDEF surfaces are in the thousands of hours. Conversely, the RCC-1 solar exposure is estimated at no more than 20 - 25 equivalent solar days, 480 - 600 hours, at least one full order of magnitude less than the LDEF. The sun exposure is a significant measure of a materials stability in that photons having energy in the range 5 - 10 eV, the solar UV, are capable of severing molecular bonds and altering materials properties.

Table 3. LDEF environmental exposure conditions.

Row	Angle off ram (degrees)	Sun Exposure (hours)	AO Fluence (atoms cm <sup>-2</sup> )
1	111.9	7,400	2.92 x 10 <sup>17</sup>
2	141.9	9,600	1.54 x 10 <sup>17</sup>
3	171.9	11,100	1.32 x 10 <sup>17</sup>
4	158.1	10,500	2.31 x 10 <sup>05</sup>
5	128.1	8,200	9.60 x 10 <sup>12</sup>
6	98.1	6,400	4.94 x 10 <sup>19</sup>
7	68.1	7,100	3.39 x 10 <sup>21</sup>
8	38.1	9,400	7.15 x 10 <sup>21</sup>
9	8.1	11,200	8.99 x 10 <sup>21</sup>
10	21.9	10,700	8.43 x 10 <sup>21</sup>
11	51.9	8,500	5.61 x 10 <sup>21</sup>
12	81.9	6,800	1.33 x 10 <sup>21</sup>
Earth	90.8	4,500	3.33 x 10 <sup>20</sup>
Space	89.2	14,500	4.59 x 10 <sup>20</sup>

### 3.2 Neutral Density and Atomic Oxygen Fluence

It is well established that variations in solar activity induce changes in the local atmospheric density at spacecraft orbital altitudes. Variations in atomic oxygen (AO) density as a function of F10.7, as predicted by the US Mass Spectrometer Incoherent Scatter (MSIS) model, are illustrated in Figure 6.<sup>5</sup> Knowledge of F10.7 variations during the LDEF mission provide detailed knowledge of atmospheric density which, when coupled with knowledge of the LDEF attitude, yield AO fluence according to the relation

$$\Phi_{AO} (\text{cm}^{-2}) = \int_0^T k_a n_{AO} v_o dt$$

where  $v_o$  (cm/s) is the orbital velocity of the spacecraft,  $n_{AO}$  ( $\text{cm}^{-3}$ ) is the number density of atomic oxygen, and  $k_a$  is an angle factor taking into account the orientation of the sample plane relative to the velocity vector, and T is the exposure duration. Performing these estimates for the LDEF yield the results indicated in Table 3.

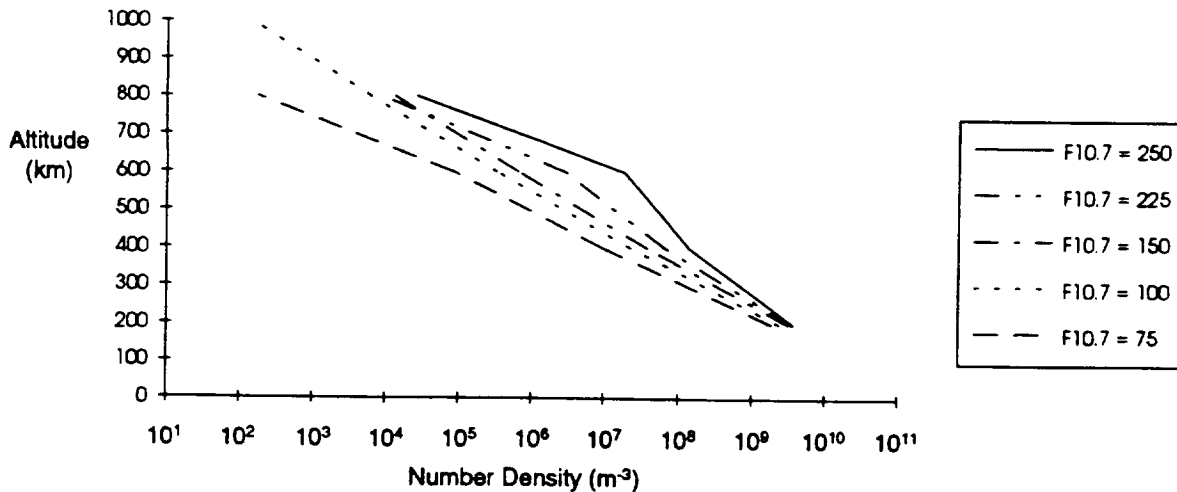


Figure 6. Atomic oxygen density as predicted by the U.S. MSIS atmospheric model.

For RCC-1, the coefficient  $k_a$  was calculated based on knowledge of the Mir OS attitude control modes and  $n_{AO}$  was based on a Russian atmospheric model. The primary attitude control mode during the course of the experiment is referred to as ICS-2. In this orientation, the y-axis of the station is normal to the orbital plane and the x-axis is parallel to the solar vector projection to the orbital plane. This mode was maintained about 50% of the flight time. A second attitude control mode used during the experiment is referred to as ICS-1. In this orientation, the x-axis of the station is parallel to the orbital plane and the y-axis is parallel to the solar vector projection. This mode was maintained about 25% of the flight time. A combination of the ICS-1 and ICS-2 modes

was used approximately 20% of the time with planned attitude control modes making up the remaining 5%. As is seen in Figure 3, the cassette was shielded by the attached module. Similarly, when the Soyuz TM and Progress transport vehicles were docked with the Mir, the RCC-1 was subject to their additional shielding effects. The calculations made by the analysis team showed that the total time of RCC-1 exposure to AO was 188 days and the mean value of  $\cos \alpha_a$  was 0.051. The integrated fluence of AO to the RCC-1 was estimated at  $5.36 \times 10^{22} \text{ cm}^{-2}$  as shown in Table 4. Consequently, the RCC-1 exposure exceeds the exposure of any LDEF surfaces by at least a factor of five.

**Table 4. Solar activity and atomic oxygen flux during the RCC-1 experiment.**

Exposure Time (hr)	Solar Activity (F10.7)	AO Flux ( $\text{cm}^{-2} \text{ s}^{-1}$ )
0	279	$1.50 \times 10^{15}$
1,000	284	$1.6 \times 10^{15}$
2,000	285	$1.65 \times 10^{15}$
3,000	286	$1.7 \times 10^{15}$
4,000	281	$1.6 \times 10^{15}$
5,000	275	$1.5 \times 10^{15}$
6,000	269	$1.4 \times 10^{15}$
7,000	264	$1.3 \times 10^{15}$
8,000	259	$1.2 \times 10^{15}$
9,000	255	$1.15 \times 10^{15}$
10,000	250	$1.0 \times 10^{15}$
11,000	246	$0.8 \times 10^{15}$
11,280	245	$0.75 \times 10^{15}$
Average	267.5	$1.32 \times 10^{15}$
Integrated Fluence = $5.36 \times 10^{22} \text{ cm}^{-2}$		

The relation between atmospheric density and F10.7, as predicted by the Russian model, is illustrated in Figure 7. The disagreement between the neutral density as predicted by the MSIS and Russian models is highlighted in Figure 8. Recall that the Russian prediction of F10.7 for the time of the RCC-1 experiment was 267.5, while the US results indicate a value closer to 200. Utilizing the Russian atmospheric model and lowering the F10.7 value from 267.5 to 200 would reduce the equivalent AO fluence to RCC-1 by about 10%. Using the AO density values predicted by the MSIS model at F10.7 = 200 would reduce the AO fluence by a factor of 5. This would bring the RCC-1 fluence into general agreement with the exposure seen by rows 9 and 10 on LDEF.

### 3.3 Radiation Environment and Absorbed Dose

During the course of the LEO experiments the sample materials were subjected to radiation from the trapped radiation belts, solar protons, and galactic cosmic rays. Because of their low altitude, both the LDEF and the RCC-1 were below most of the trapped radiation belts save for the region referred to as the South Atlantic Anomaly. This phenomena provided most of the ionizing radiation that the LDEF and RCC-1 were exposed to as the Earth's magnetic field effectively screened the majority of the solar protons and galactic cosmic rays.

The flux of electrons and protons to both spacecraft was calculated based on two separate isotropic flux distribution models. The radiation belt fluences for both the LDEF and RCC-1 missions are illustrated in Figure 9. Note that even though the RCC-1 mission was significantly shorter than that of the LDEF its fluence is greater because of its higher orbital inclination. These fluence values are listed in Table 5.

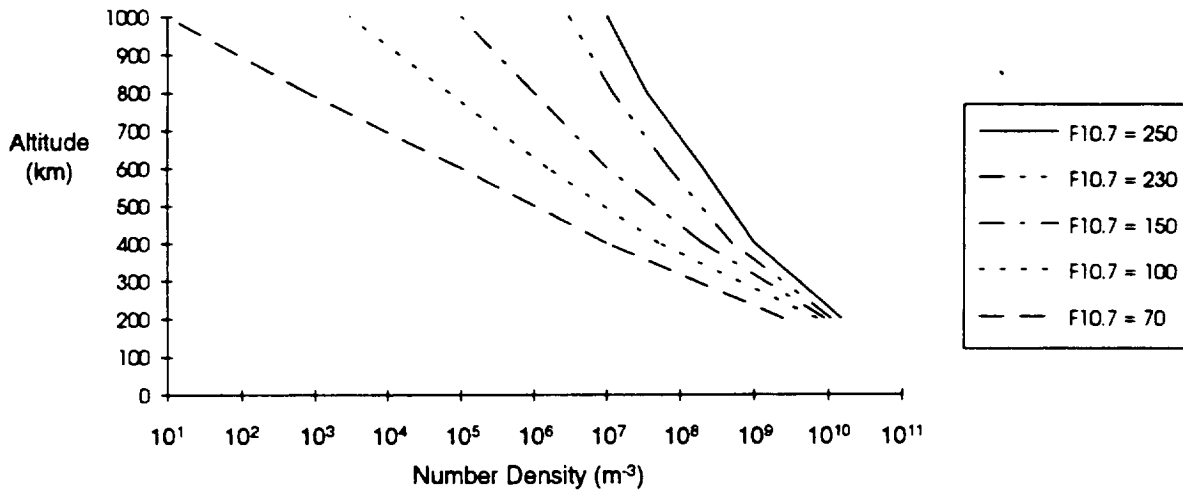


Figure 7. Atomic oxygen density as predicted by the Russian atmospheric model.

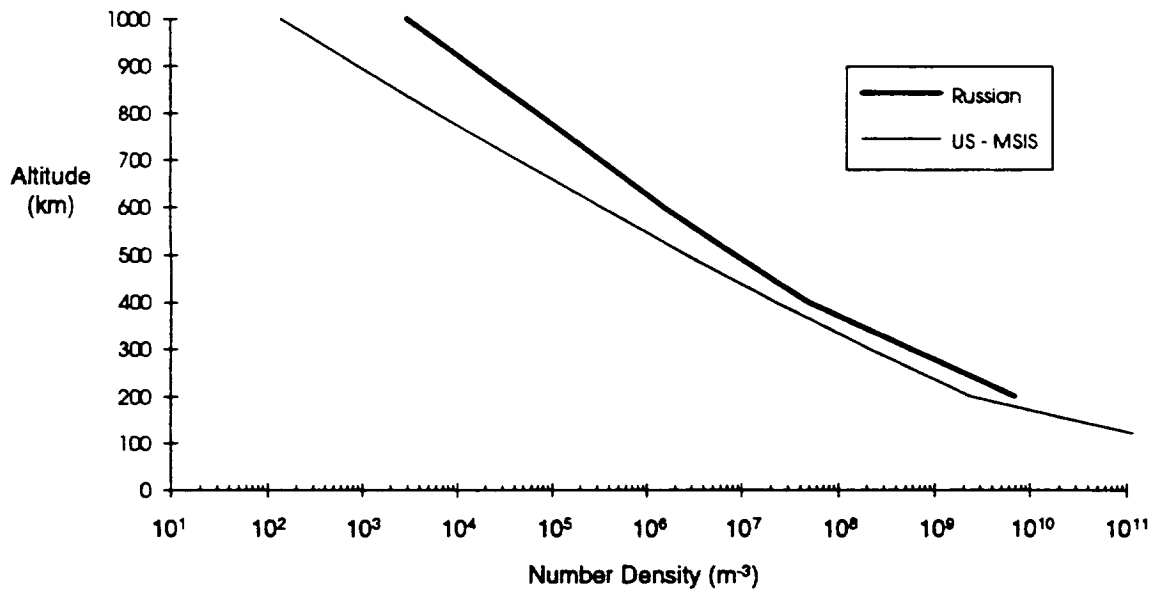


Figure 8. Comparison of US and Russian atmospheric density for F10.7 = 100.

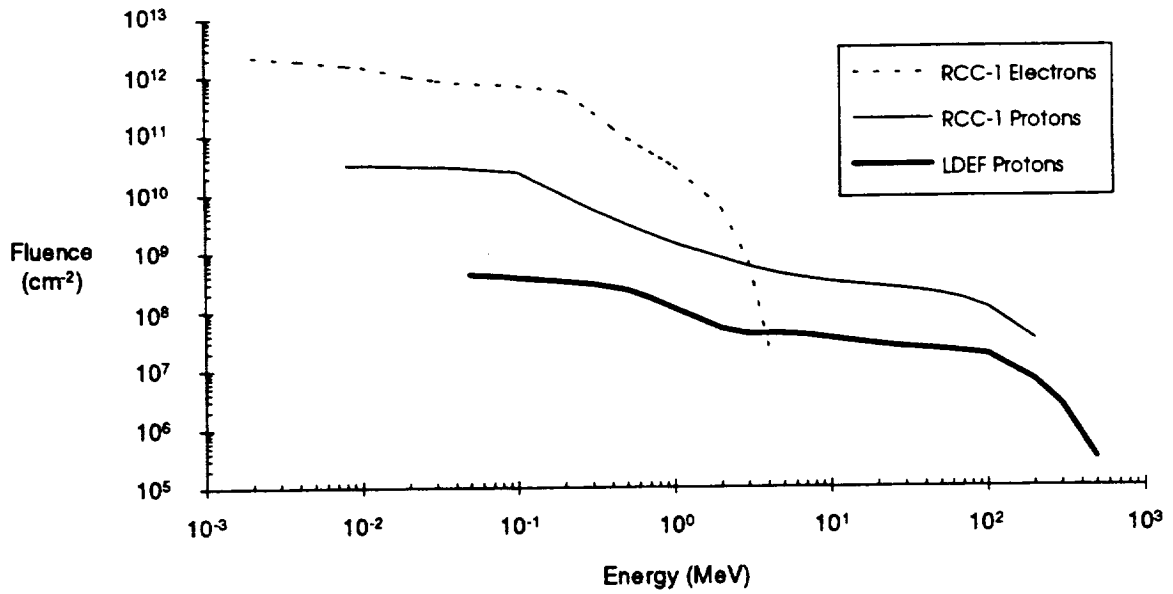


Figure 9. Proton and electron belt fluence predictions for the LDEF and RCC-1 experiments.

Table 5. Russian proton and electron belt fluence predictions for the RCC-1 experiment

Proton Flux		Electron Flux	
Energy (MeV)	Fluence (x 10 <sup>9</sup> cm <sup>-2</sup> )	Energy (MeV)	Fluence (x 10 <sup>9</sup> cm <sup>-2</sup> )
0.008	31.7	0.002	2140
0.010	31.4	0.004	1860
0.020	29.9	0.008	1540
0.040	28.4	0.010	1450
0.080	24.7	0.020	983
0.100	23.7	0.030	843
0.300	5.36	0.040	757
0.500	2.99	0.100	671
0.700	2.06	0.200	570
1.000	1.42	0.300	240
3.000	0.563	0.400	132
5.00	0.413	0.500	87.3
7.00	0.350	0.600	64.2
10.0	0.304	0.700	50.3
30.0	0.225	0.800	40.8
40.0	0.205	0.900	33.8
50.0	0.186	1.00	28.5
70.0	0.151	2.00	5.61
100.0	0.108	3.00	0.682
200.0	0.031	4.00	0.024

The LDEF radiation dose values have been well studied and are on the order of  $3 \times 10^4$  rads as illustrated in Figure 10. The placement of the RCC-1 cassette provided partial shielding of the TCC samples to the direct effect

of the Van Allen belt (VAB) particle fluxes. Performing a Monte-Carlo simulation indicated that 26% of the overall VAB flux fell on the working side of the RCC-1 samples, with the remaining 74% of the flux impinging the opposite side of the spacecraft. The radiation dose absorbed by the RCC-1 samples is estimated at  $8 \times 10^5$  rads as shown in Table 6.

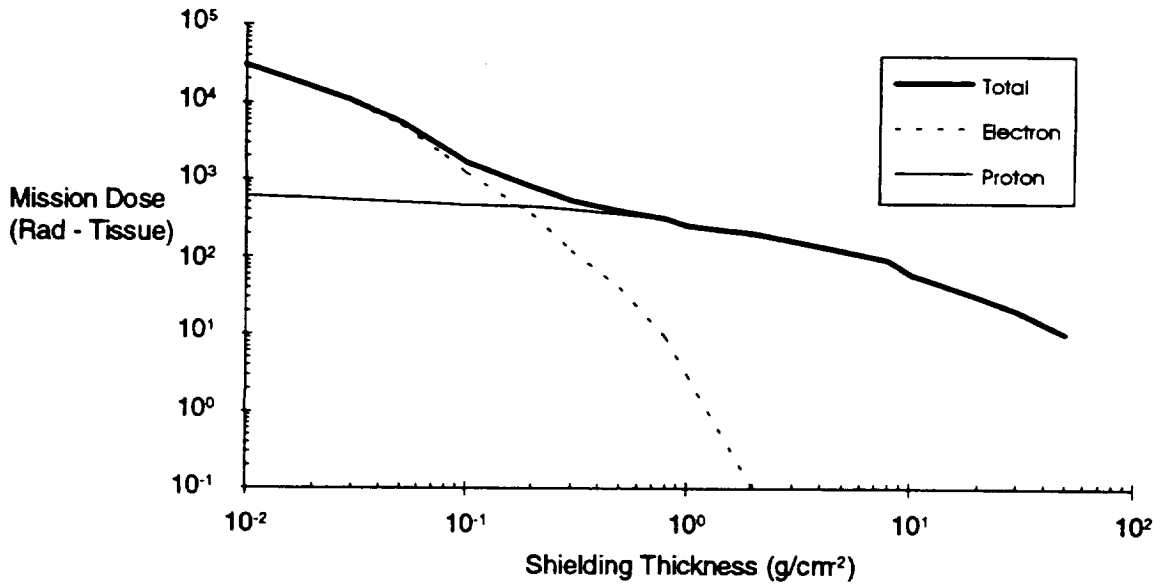


Figure 10. The LDEF mission radiation dose profile.

Table 6. Radiation dose values for the RCC-1 experiment.

Source	Dose (rad)
Trapped Protons	$2.7 \times 10^5$
Trapped Electrons	$5.3 \times 10^5$
Total	$8.0 \times 10^5$

### 3.4 Comparison of LDEF and RCC-1 Environment

The LDEF and RCC-1 orbital exposure conditions are compared in Table 7. As shown, the RCC-1 AO fluence is approximately equal to that seen by rows 9 - 10 of LDEF when determined using US models. The RCC-1 UV exposure is only about 1/20th of rows 9 and 10 of LDEF and the RCC-1 radiation dose is a factor of 25 higher. As a result, the RCC-1 experiment would not be expected to witness UV degradation in materials if the time scale associated with the degradation process were longer than ~ 500 hours. Conversely, the RCC-1 materials would be more susceptible to radiation damage. However, since these levels of radiation are not close to the usable limits for most materials, the main difference will be the UV exposure value.

**Table 7. Comparison of the LDEF and RCC-1 environmental exposure conditions.**

	LDEF		RCC-1	
	Row 9	Row 10	Russian Models	US Models
UV Exposure (hrs)	11,200	10,700	~ 600	-
AO Fluence ( $\times 10^{21}$ cm <sup>-2</sup> )	8.99	8.43	53.6	~ 10
Dose (krad)	30	30	800	-

#### 4 FLIGHT TEST RESULTS

##### 4.1 Summary of RCC-1 Thermal Control Coatings Exposure

The Russian RCC-1 TCC experiment contained 14 separate materials as listed in Table 8. As indicated, only two US materials, Z93 and YB71, bear chemical similarity to their Russian counterparts despite full functional similarity. Test were conducted on the RCC-1 materials to measure their optical, mass loss, and chemical properties. A visual inspection of the TCC samples was conducted to assess the external appearance of the samples. Solar absorptance and emissivity were measured under laboratory conditions by an applied photometer, (FM-59), and a themoradiometer, (TEPM-1), while sample mass changes were determined from pre and post-flight mass determinations using an analytical balance having an accuracy of 0.1 mg. Finally, a chemical composition analysis of the RCC-1 material surfaces was performed with the use of an x-ray dispersionless microanalyzer with a semiconductor radiation receiver built in the electronic microscope.

##### 4.1.1 Visual Inspection

Visual inspection of the TCC samples showed some significant changes in the external appearance of many of the samples as illustrated in Table 9. The AK-512-w, KO-5258, and 40-1-12-88 reflectors changed from white to various shades of yellow. The unprotected absorber AK-243 changed from black-mat to grayish-blue. This is probably due to AO erosion of the acrylic resin binder. The grayish-blue could be easily rubbed out but surface mat color loss was observed. The FP-5246 coating changed from black to grayish-white. The protected absorbers showed no change in color or state. The AK-512-g changed from dark green to emerald green with more mat surface. All other materials showed no visible change.

##### 4.1.2 Surface Morphology

Magnified images of four of the coatings were obtained with the use of an electron microscope, Figures 11 - 13. Investigation of the surface structure indicated that the ceramic and paint coatings vary in surface relief. Before the flight the enamels had a rather flat surface with a small number of pores. After exposure to space, the paint coating surface appeared rougher and the number of pores increased. Before flight, the ceramic coatings already had a large number of cracks on their surfaces. After flight both the number and dimension of cracks were

Table 8. Thermal control coating materials exposed on the RCC-1 experiment.

Class	Reference	Chemical Nature	Max. Temp. (C)	US Equivalent	
				Chemical	Functional
Reflector	AK-512-w	TiO <sub>2</sub> + ZnO / acrylic resin	60 - 72	-	A276, S13G, YB-71, Z93
	KO-5191	ZnO / silicone resin	72 - 90	-	"
	KO-5258	ZnO + TiO / silicone resin	60 - 72	-	"
	TP-co-2	ZnO / potassium metasilicate	50 - 60	Z93	"
	TP-co-10M	ZnO / asbestos	60 - 72	-	"
	TP-co-11	ZnO / orthotitanate - potassium metasilicate	50 - 60	YB71	"
	TP-co-12	ZnO / potassium metasilicate	< 40	Z93	"
	TP-co-90	Zr Titanate / potassium metasilicate	< 40	-	"
	40-1-12-88	ZrO <sub>2</sub> / silicone resin	60 - 72	-	"
	Absorber	AK-243	deep black pigment / acrylic resin	72 - 90	-
FP-5246		deep black pigment / fluoroplastic solution	72 - 90	-	"
Other	AK-512-g	CrO / silicone resin - green	72 - 90	-	n/a
	AMr-6 (w)	acid anodized aluminum - white	50 - 60	-	anodized aluminum
	AMr-6 (b)	acid anodized aluminum - black	72 - 90	-	anodized aluminum

observed to have increased, probably due to thermal cycling. The surface relief of the coating TP-co-10M, which showed no evidence of a contaminant layer, did not vary. The egress of pigment particles on the surface of coatings TP-co-90 and 40-1-12-88 is easily seen. In this case the degree of the surface filling with such particles is insignificant. This fact correlates with the results of chemical analysis of these TCC which shows a decrease in surface pigment and an increase in surface binder.

**Table 9. Visual inspection of the RCC-1 thermal control coating materials.**

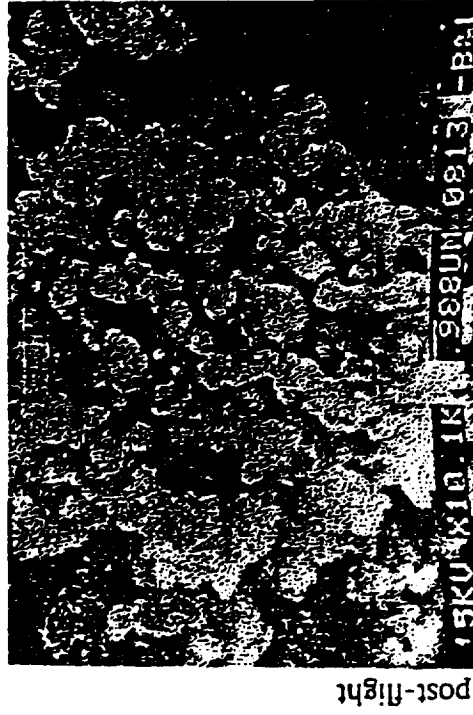
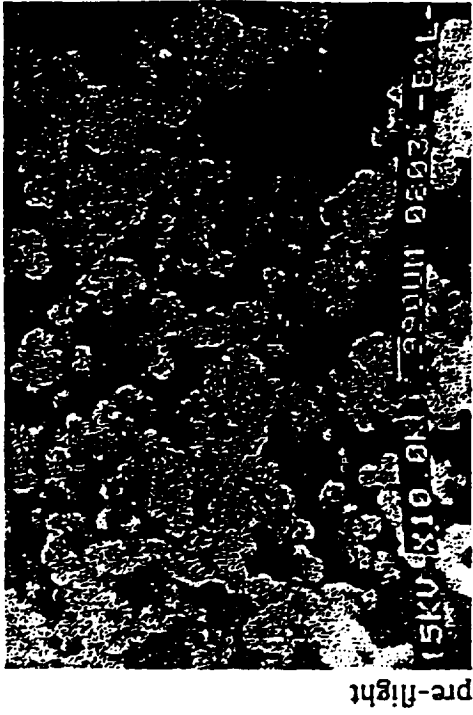
Class	Reference	Final Appearance
Reflectors	AK-512-w	gray-yellow
	KO-5191	no change
	KO-5258	gray-yellow
	TP-co-2	no change
	TP-co-10M	no change
	TP-co-11	no change
	TP-co-12	no change
	TP-co-90	no change
	40-1-12-88	bright yellow
Absorbers	AK-243*	grayish-blue
	FP-5246*	grayish-white
Other	AK-512-g	initial: dark green final: emerald green
	AMr 6 (w)	no change
	AMr 6 (b)	no change
*samples protected by quartz glass did not exhibit a change in surface color		

#### 4.1.3 Optical Properties

Laboratory measurements of solar absorptance, emittance, and mass loss for the TCCs are given in Table 10. A number of TCC materials did not experience any significant changes in solar absorptance or emittance and showed no significant mass changes. This proves the stability of these coatings under exposure to the space environment. The TP-co-2, TP-co-11, and TP-co-12 coatings are the most stable, while KO-5191 exhibited the highest increase in solar absorptance, (0.02), due to the degrading effect of the solar UV.

White paint 40-1-12-88 turned out to be the least stable material studied. This material is based on ZrO<sub>2</sub> and is known to be very sensitive to UV radiation. Because this material exhibited no practical mass change it can be concluded that it is relatively immune to AO attack, thereby preventing any cleaning erosion effect. Conversely, the coatings TP-co-10M and TP-co-90 showed a mass decrease, but no change in optical properties. This is consistent with the optical stability of these materials was maintained by AO erosion on the exterior surface. No significant changes in emittance were observed for any of the materials.

10' x magnification



300 x magnification

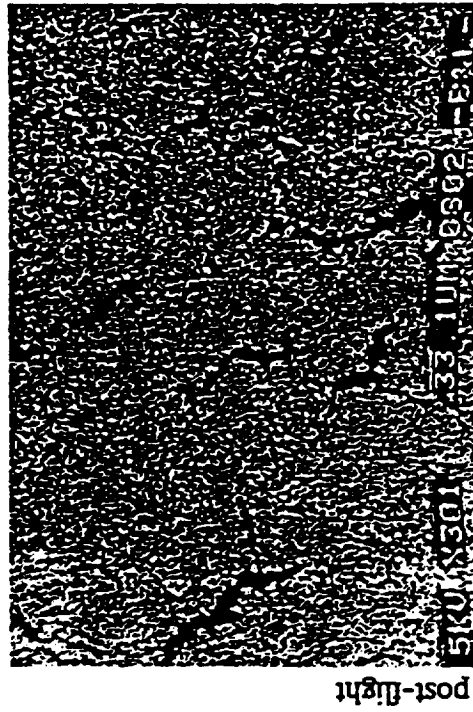
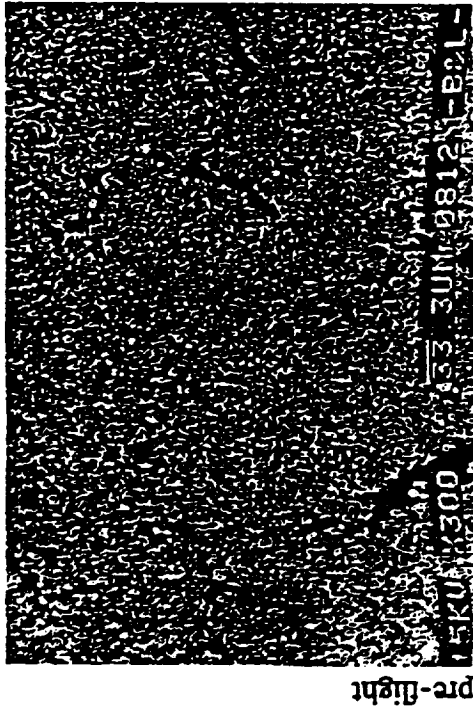
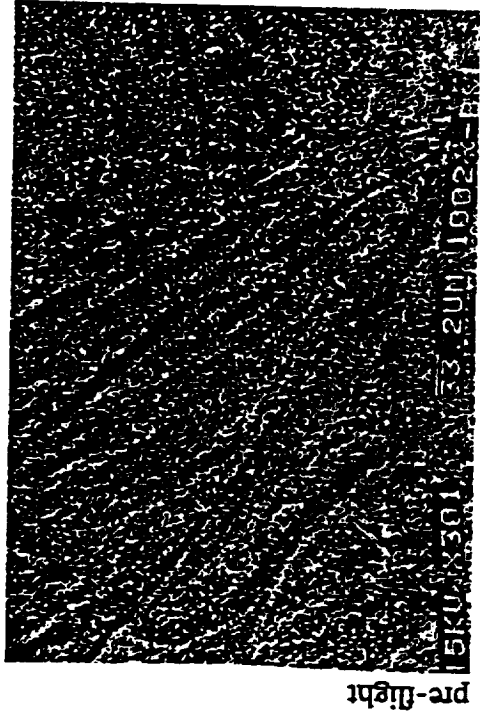


Figure 11. Surface morphology of the TP-co-10M coating.

NPO ENERGIA

300 x magnification



10' x magnification

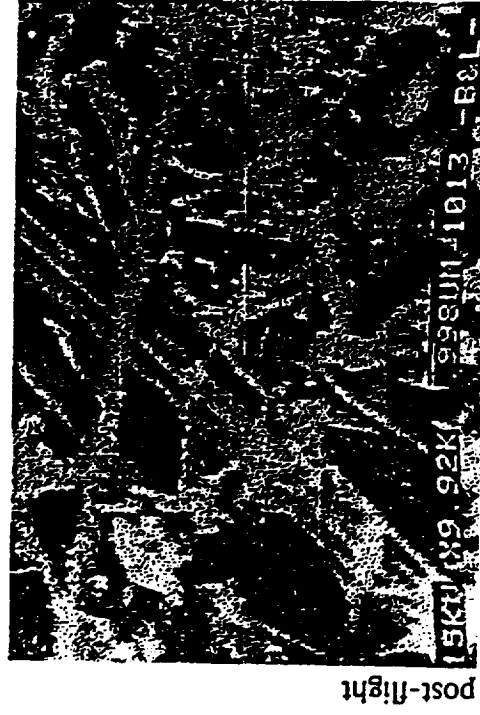
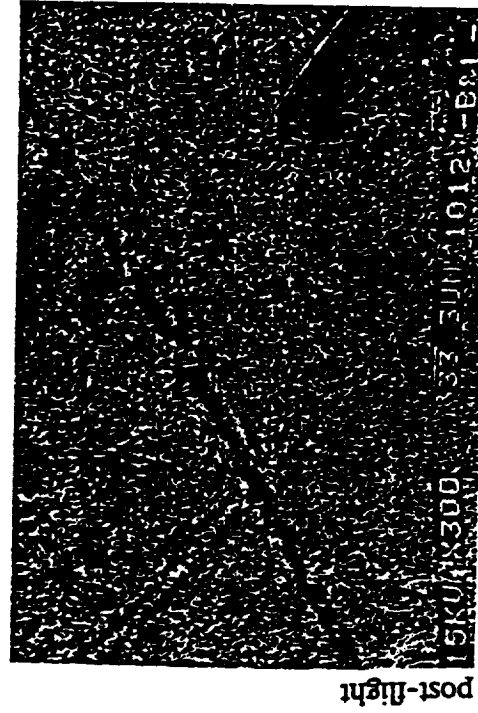
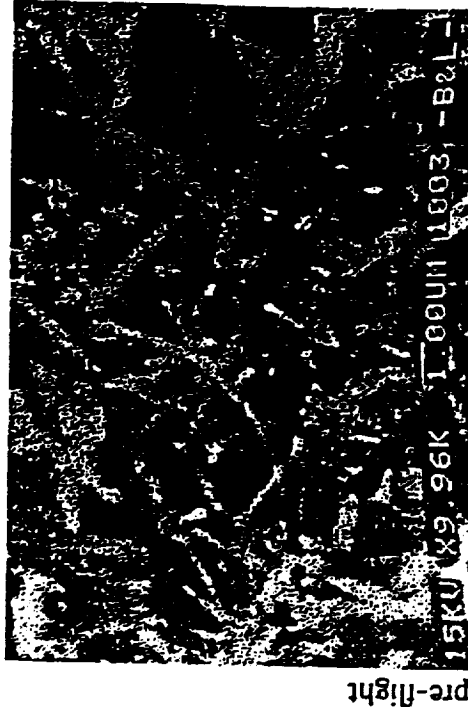
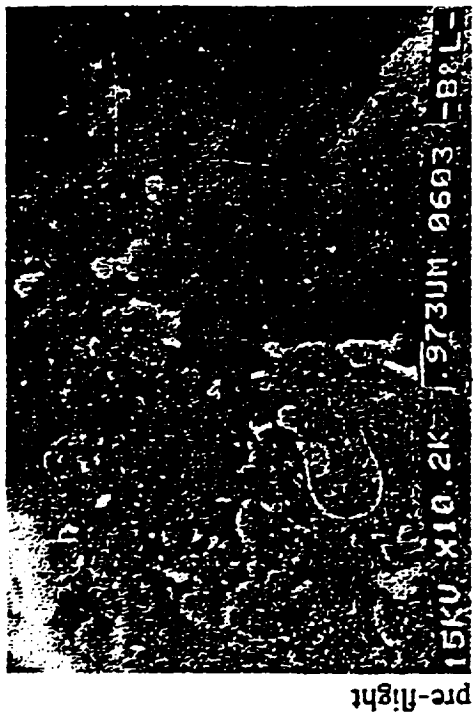


Figure 12. Surface morphology of the TP-co-12 coating.

40-1-12-88



TP-co-90

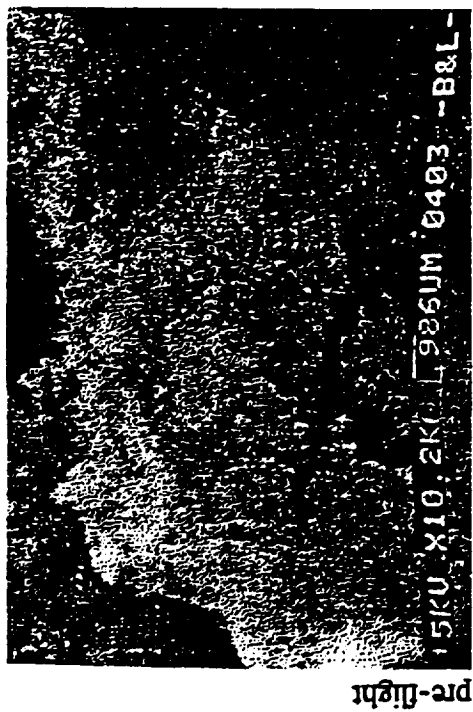


Figure 13. Surface morphology of the TP-co-90 and 40-1-12-88 coatings.

Table 10. Full scale test results of the RCC-1 thermal control coating materials.

Class	Reference	Absorptance		Emittance		Mass (g)		$\Delta m$ (mg)		
		Pre-Flight	Post-Flight	$\Delta\alpha$	Pre-Flight	Post-Flight	$\Delta\epsilon$		Pre-Flight	Post-Flight
Reflector	AK-512-w	0.30	0.30	0.00	0.88	0.88	0.00	4.3844	4.3837	-0.7
	KO-5191	0.18	0.20	0.02	0.89	0.89	0.00	4.5258	4.5258	0.0
	KO-5258	0.27	0.31	0.04	0.90	0.89	-0.01	4.6203	4.6206	0.3
	TP-co-2	0.18	0.18	0.00	0.97	0.94	-0.03	4.6200	4.6197	-0.3
	TP-co-10M	0.20	0.20	0.00	0.84	0.84	0.00	4.6992	4.6973	-1.9
	TP-co-11	0.14	0.14	0.00	0.93	0.91	-0.02	4.5807	4.5807	0.0
	TP-co-12	0.19	0.19	0.00	0.96	0.94	-0.02	4.5260	4.5271	1.1
	TP-co-90	0.15	0.15	0.00	0.95	0.94	-0.01	4.6095	4.6068	-2.7
	40-1-12-88	0.21	0.28	0.07	0.92	0.91	-0.01	4.6222	4.6223	0.1
	Absorber	AK-243	0.98	0.92	-0.06	0.95	0.94	-0.01	4.3839	4.3784
AK-243*		0.98	0.97	-0.01	0.95	0.95	0.00	4.3619	4.3608	-1.1
FP-5246		0.98	0.96	-0.02	0.92	0.91	-0.01	4.3783	4.3717	-6.6
FP-5246*		0.98	0.98	0.00	0.92	0.91	-0.01	4.4102	4.4099	-0.3
Other	AK-512-g	0.83	0.75	-0.08	0.91	0.91	0.00	4.4623	4.4586	-3.7
	AMr 6 (w)	0.19	0.22	0.03	0.78	0.78	0.00	3.9240	3.9241	0.1
	AMr-6 (b)	0.94	0.94	0.00	0.92	0.91	-0.01	3.9563	3.9559	-0.4

\*Protected by quartz glass

#### 4.1.3.1 UV/Visible Reflectance Properties

Measurements of the diffuse reflection spectra, ( $\rho_\lambda$ ), in the range 350 - 850 nm are given for each of the TCCs in Figures 14 - 27.

AK-512-w, (Figure 14), and KO-5191, (Figure 15), did not experience changes save in the ultraviolet region, 370 - 450 nm. AK-512-w displayed a maximum 8% increase and KO-5191 displayed a maximum 4% decrease. The abnormal behavior of the AK-512-w coating could be caused by: i) an increase in the fraction of pigment on the coating surface, ii) a change in the sample surface relief, or iii) a change of the electrical state of the pigment.

The KO-5258 coating, (Figure 16), which included the zinc oxide and titanium dioxide mixture, turned out to be the least resistant to space exposure. This indicates that the simultaneous inclusion of both ZnO and TiO<sub>2</sub> pigments is less effective than the use of either of them singly.

The silicate coatings TP-co-2, (Figure 17), TP-co-11, (Figure 19), TP-co-12, (Figure 20), and TP-co-90, (Figure 21), exhibited a slight change, (~ 2%), in reflection for wavelengths less than 400 nm. This is also true for the asbestos coating TP-co-10M, (Figure 18). Changes in the visible and shortwave infrared spectra were not detected. As expected, the 40-1-12-88 coating, (Figure 22), experienced the greatest change in  $\rho_\lambda$ . The sample color had changed from white to yellow-brown during the mission. The differential reflection spectrum extends over the spectral interval 270 to 700 nm, exceeding 50% at 400 nm. The instability is attributed to the use of an unstable polymer as a binding agent in this enamel.

The unprotected samples of AK-243 and FP-5246, (Figures 23 and 24), were noticeably discolored and their  $\rho_\lambda$  values increased. The color and  $\rho_\lambda$  of the protected samples remained virtually unchanged, (Figures 25 and 26). The AK-512-g coating, (Figure 27), showed the largest degree of discoloration and  $\rho_\lambda$  increase.

#### 4.1.3.2 IR Reflectance Properties

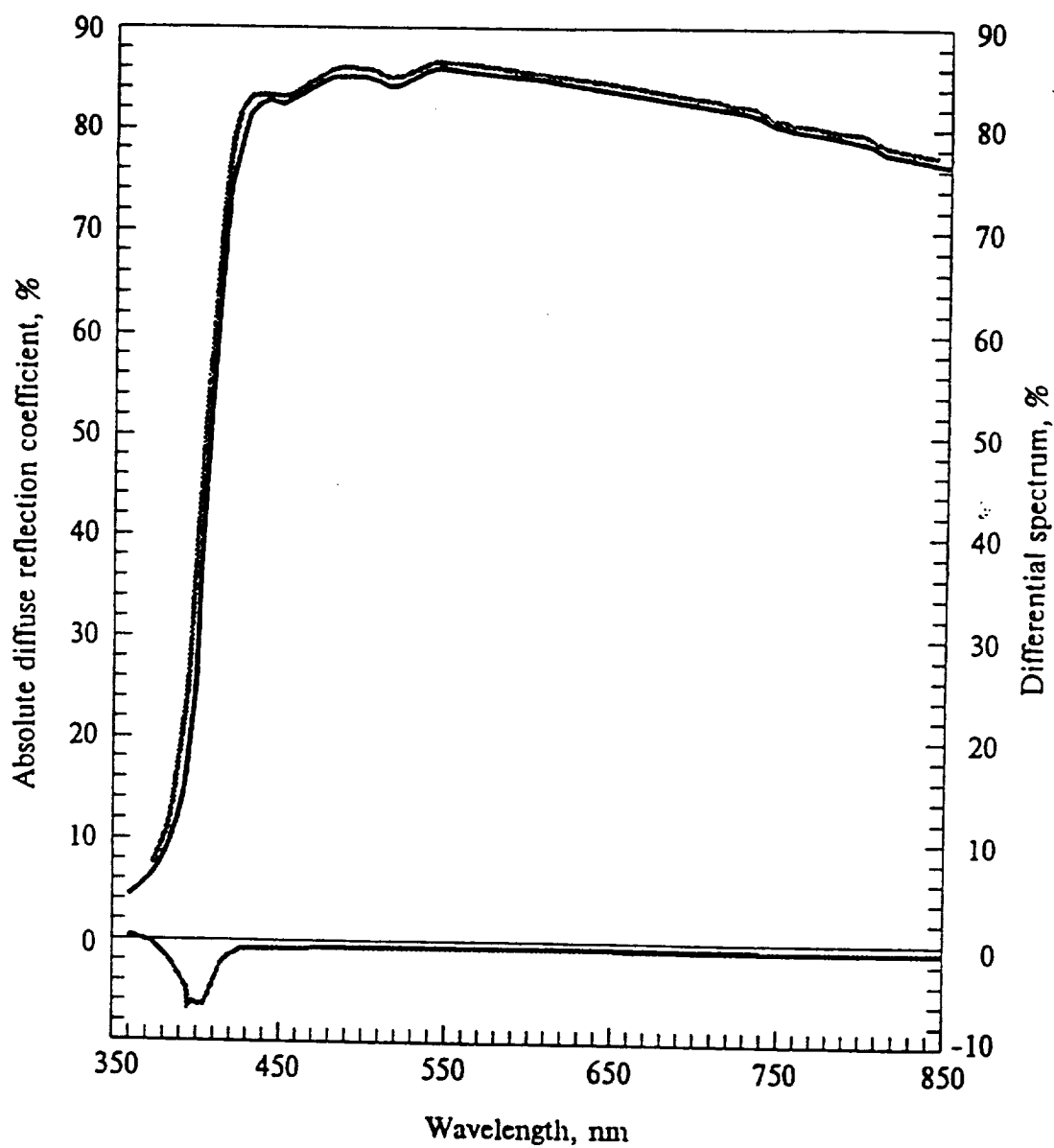
Measurements of  $\rho_\lambda$  in the range 1000 - 2500 nm are provided in Figures 28 - 38. All reflectors showed a slight decrease in  $\rho_\lambda$  except for TP-co-11, (Figure 33), and TP-co-12, (Figure 34), samples which showed a minor increase. The TP-co-10M coating showed the largest change, exhibiting a 3% decrease at approximately 1850 nm.

The reflection spectra for the absorption coatings FP-5246, (Figure 37), and AK-243 (Figure 36) both increased after exposure. The AK-512-g, (Figure 38), spectra increased almost uniformly by approximately 10%. The increase was greater for the unprotected samples than for the protected ones, with the AK-243 post-flight increase being the greatest. The AK-243 increase occurred mainly at the shorter wavelengths while the FP-5246 changes were at the longer wavelengths. This may indicate a change in the coating binder.

#### 4.1.4 Mass Loss

Mass loss was observed on the majority of the samples due to erosion by AO, see Table 10. The greatest mass loss was observed on the black paint FP-5246 and is related to the carbon content in the coating pigment binder which is susceptible to AO. KO-5191 and TP-co-11 demonstrated no mass changes, while the porous ceramic coating TP-co-12 demonstrated a significant increase of 1.1 mg. It is believed that this increase is due to

### DIFFUSE REFLECTION SPECTRA FOR COATING AK-512



— before flight  
— after flight  
— differential spectrum

Figure 14. Diffuse UV/visible reflection spectra of the AK-512-w coating.

DIFFUSE REFLECTION SPECTRA  
FOR COATING KO-5191

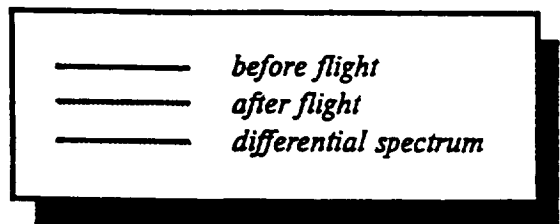
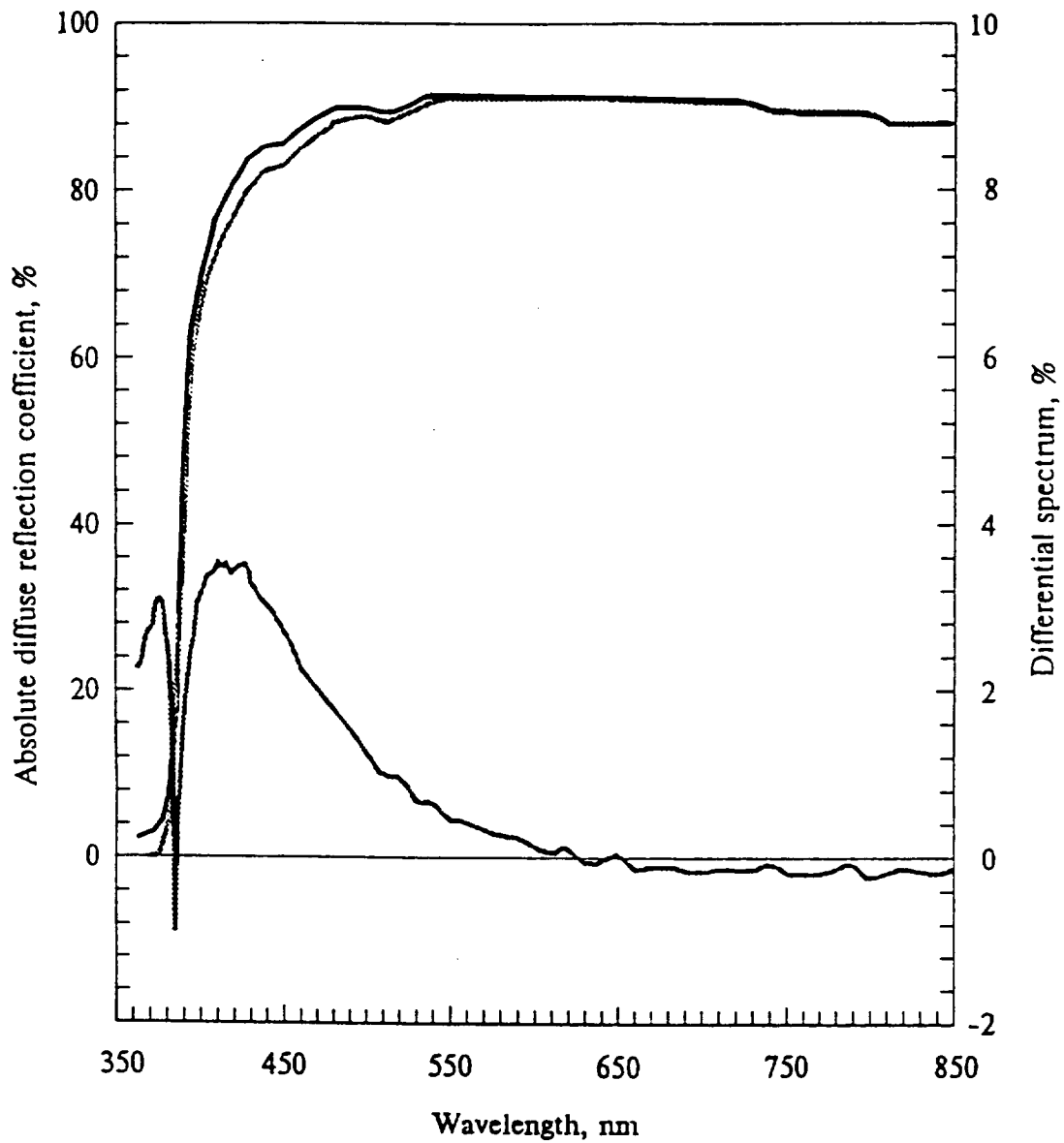
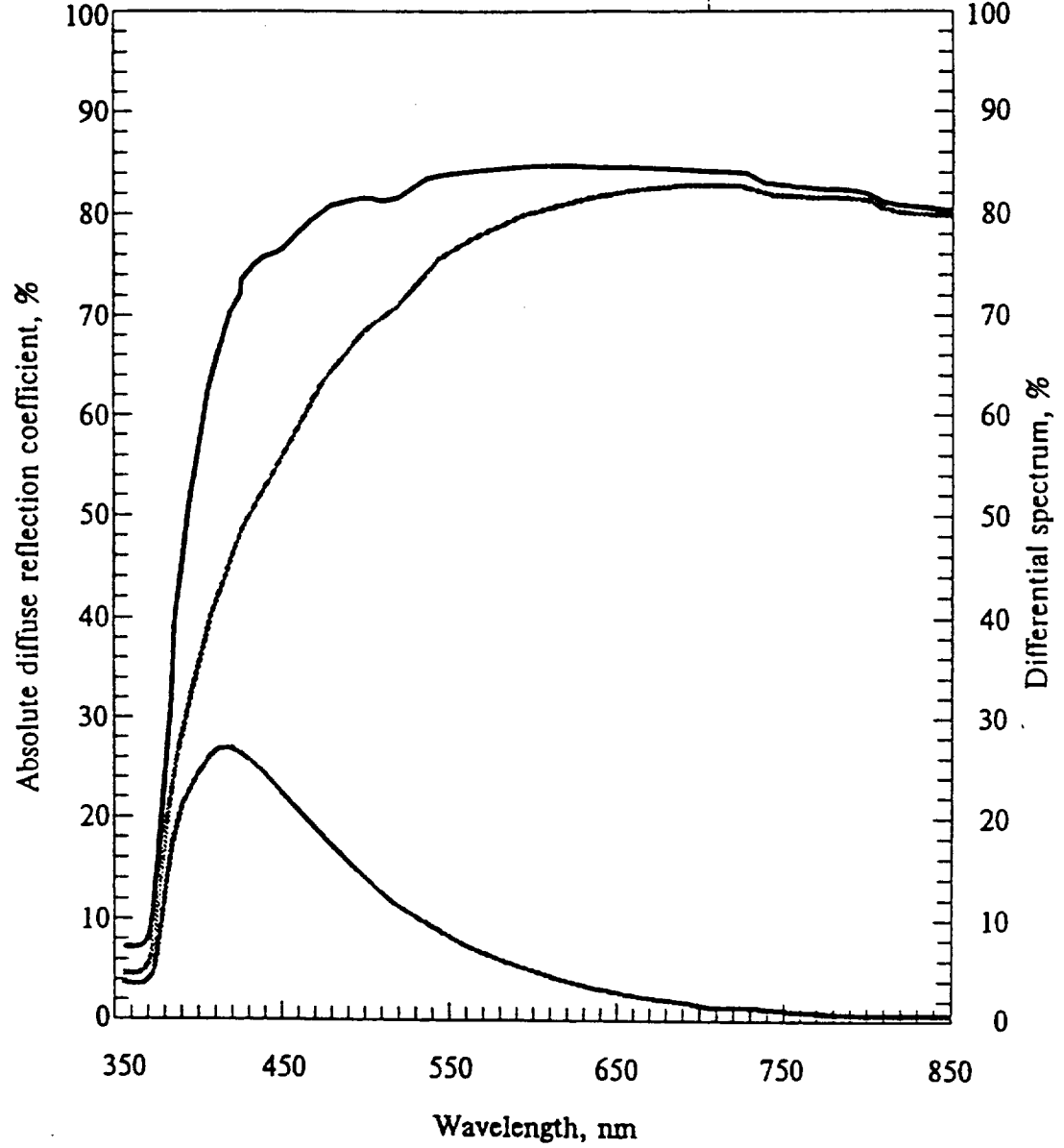


Figure 15. Diffuse UV/visible reflection spectra of the KO-5191 coating.

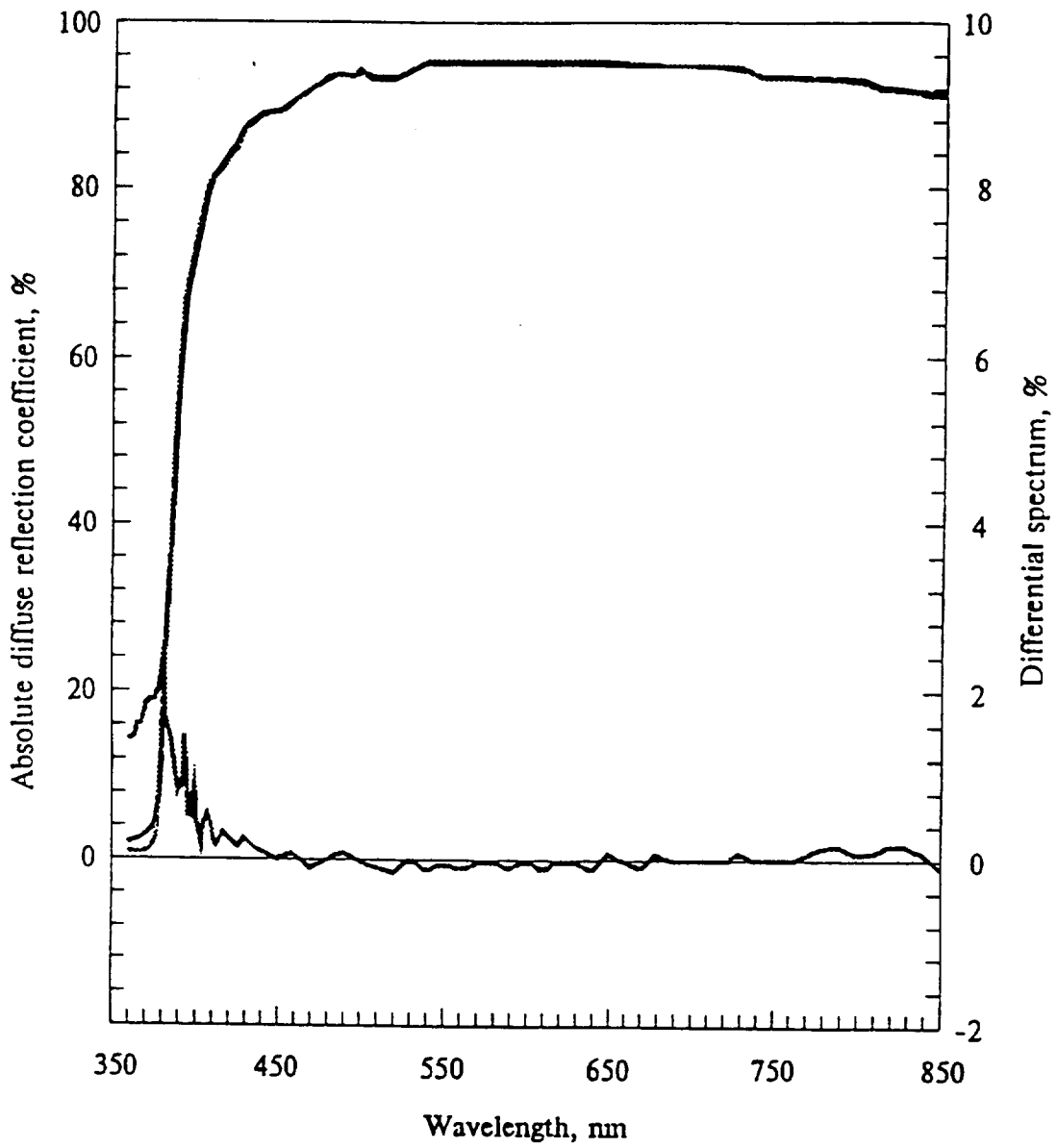
DIFFUSE REFLECTION SPECTRA  
FOR COATING KO-5258



— before flight  
— after flight  
— differential spectrum

Figure 16. Diffuse UV/visible reflection spectra of the KO-5258 coating.

### DIFFUSE REFLECTION SPECTRA FOR COATING TP-co-2



— before flight  
— after flight  
— differential spectrum

Figure 17. Diffuse UV/visible reflection spectra of the TP-co-2 coating.

DIFFUSE REFLECTION SPECTRA  
FOR COATING TP-co-10M

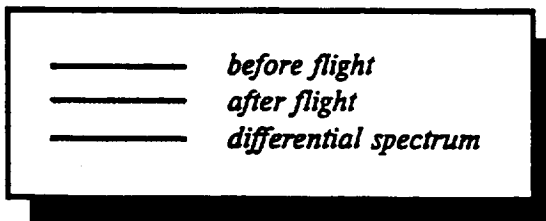
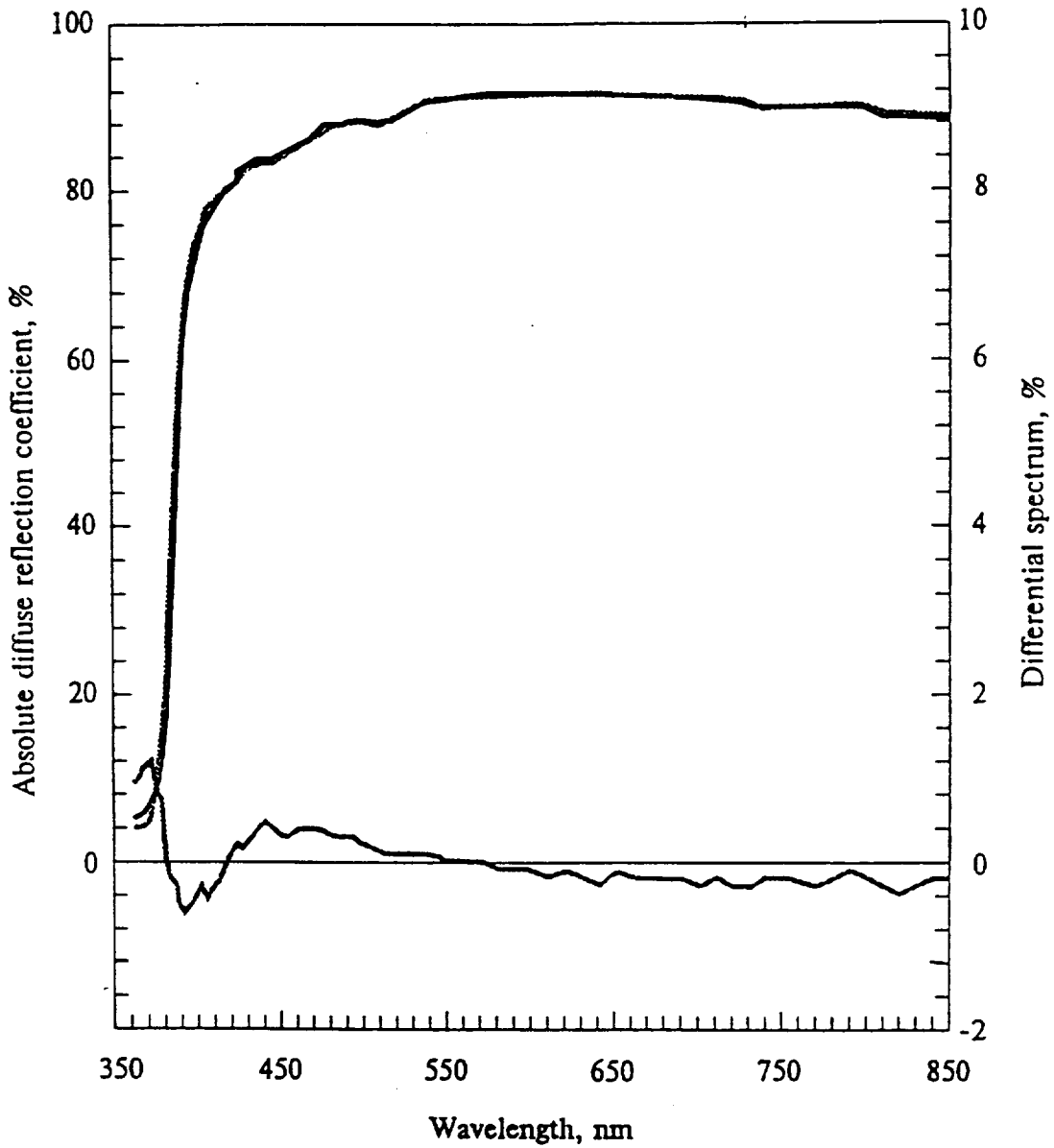


Figure 18. Diffuse UV/visible reflection spectra of the TP-co-10M coating.

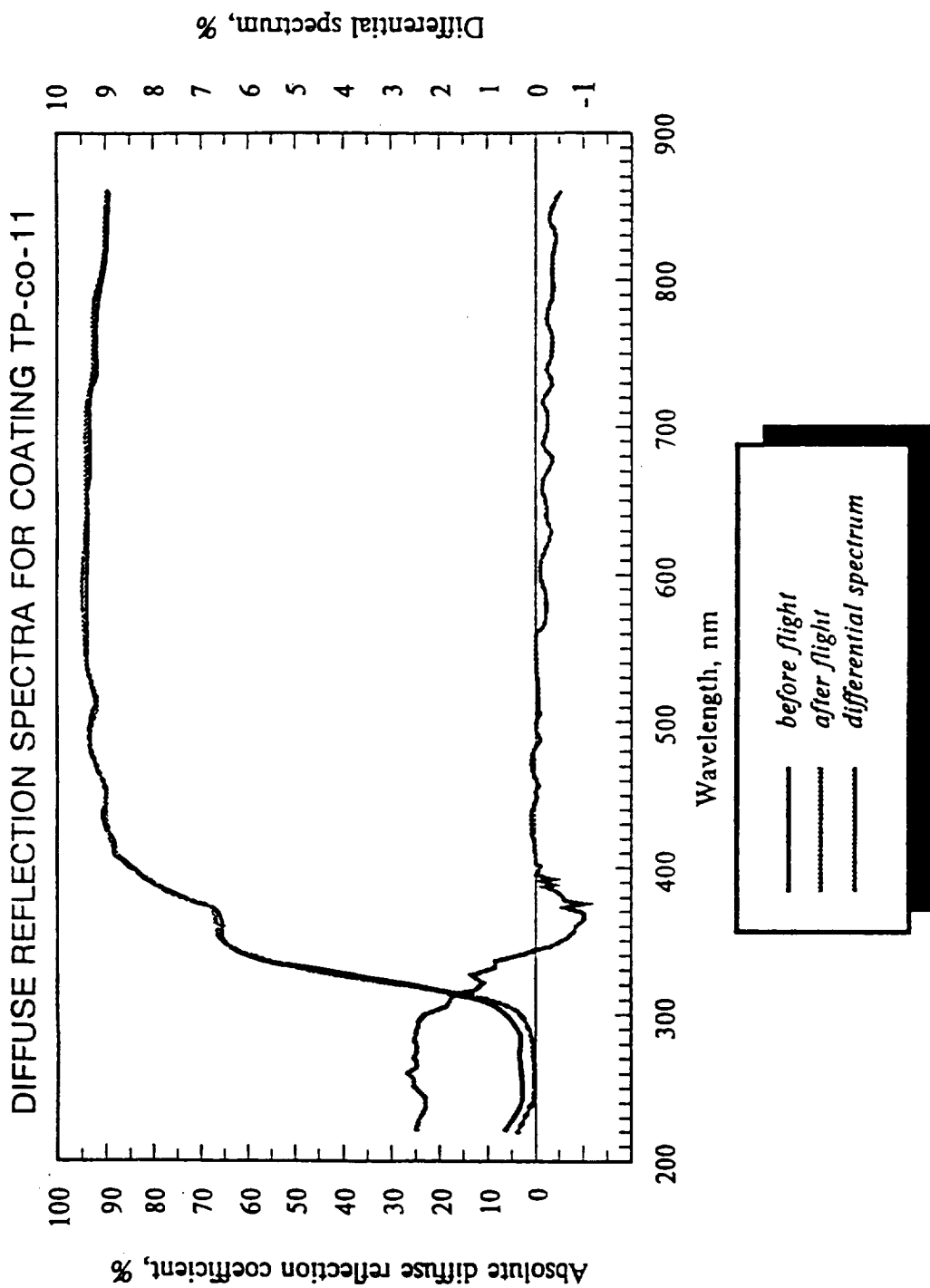


Figure 19. Diffuse UV/visible reflection spectra of the TP-co-11 coating.

DIFFUSE REFLECTION SPECTRA  
FOR COATING TP-co-12

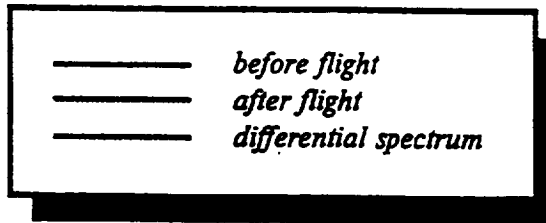
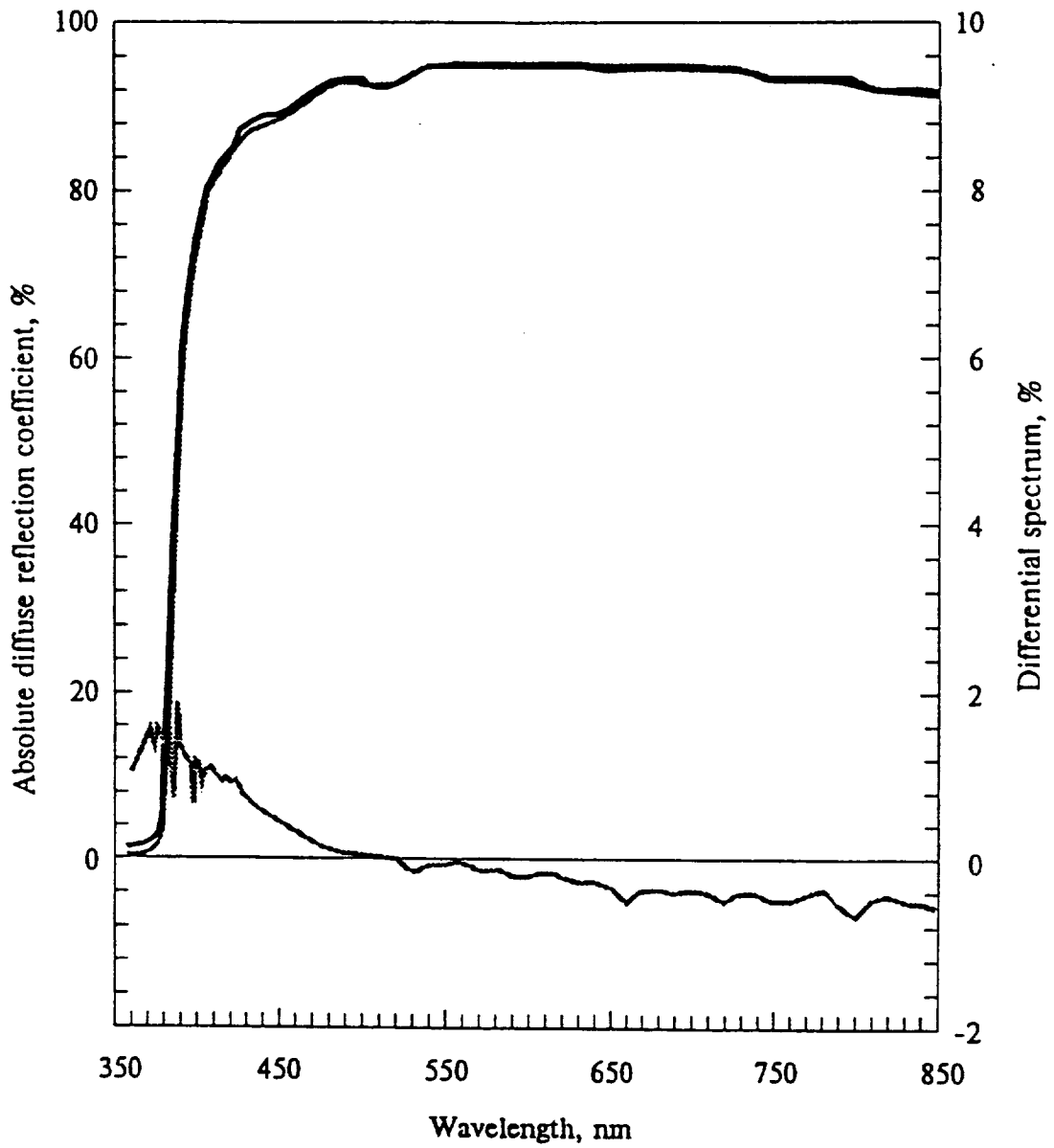


Figure 20. Diffuse UV/visible reflection spectra of the TP-co-12 coating.

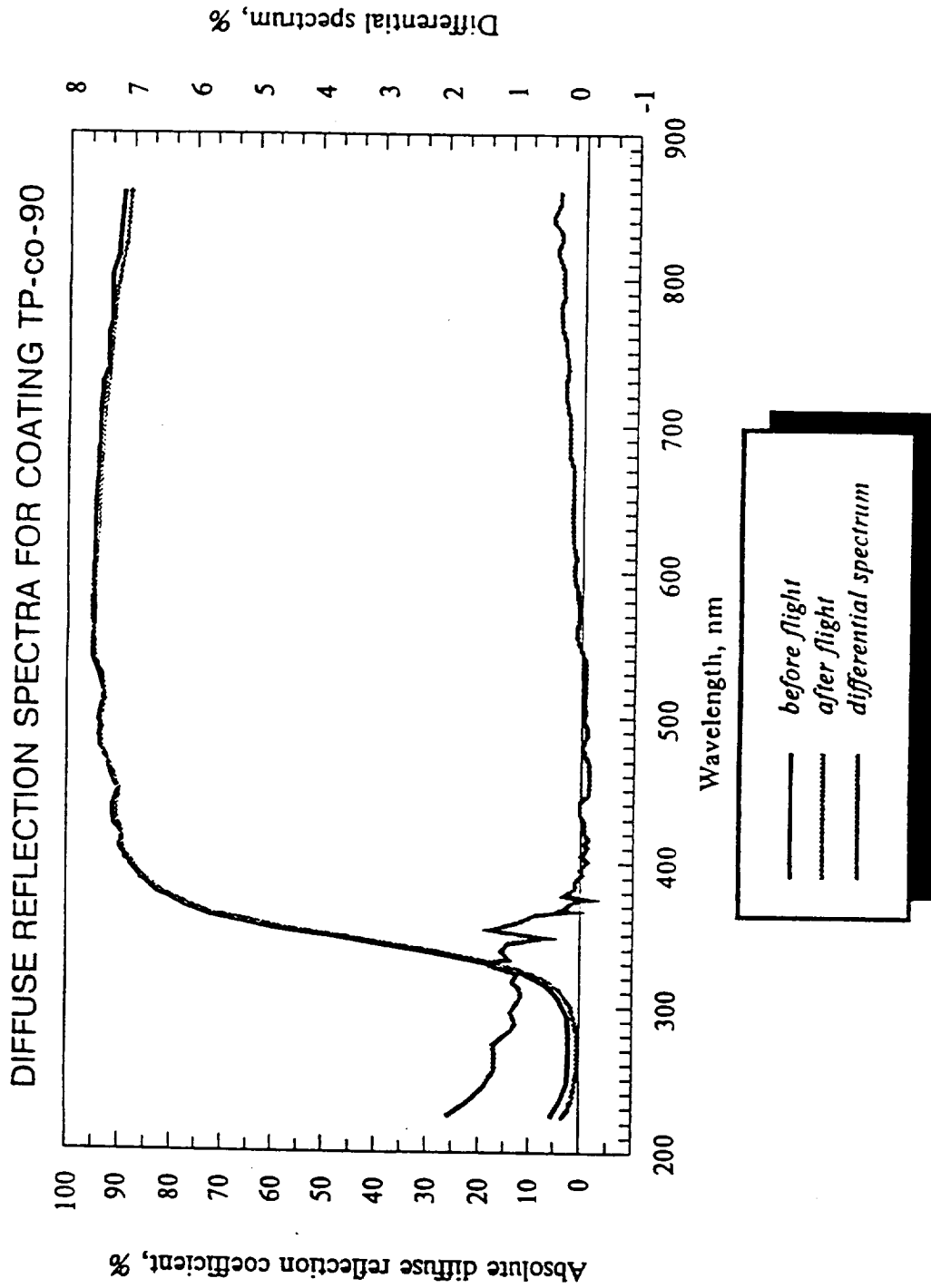


Figure 21. Diffuse UV/visible reflection spectra of the TP-co-90 coating.

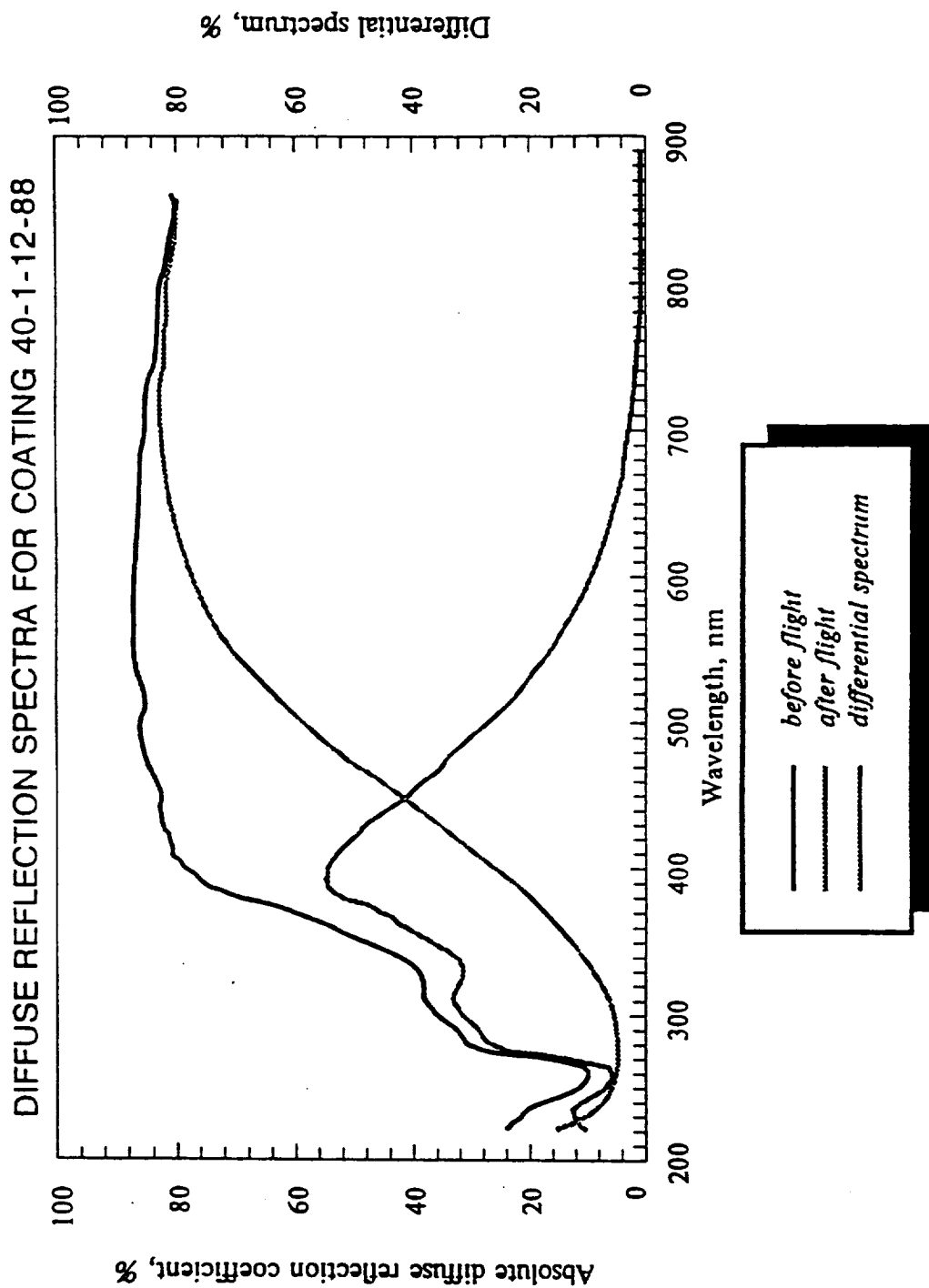
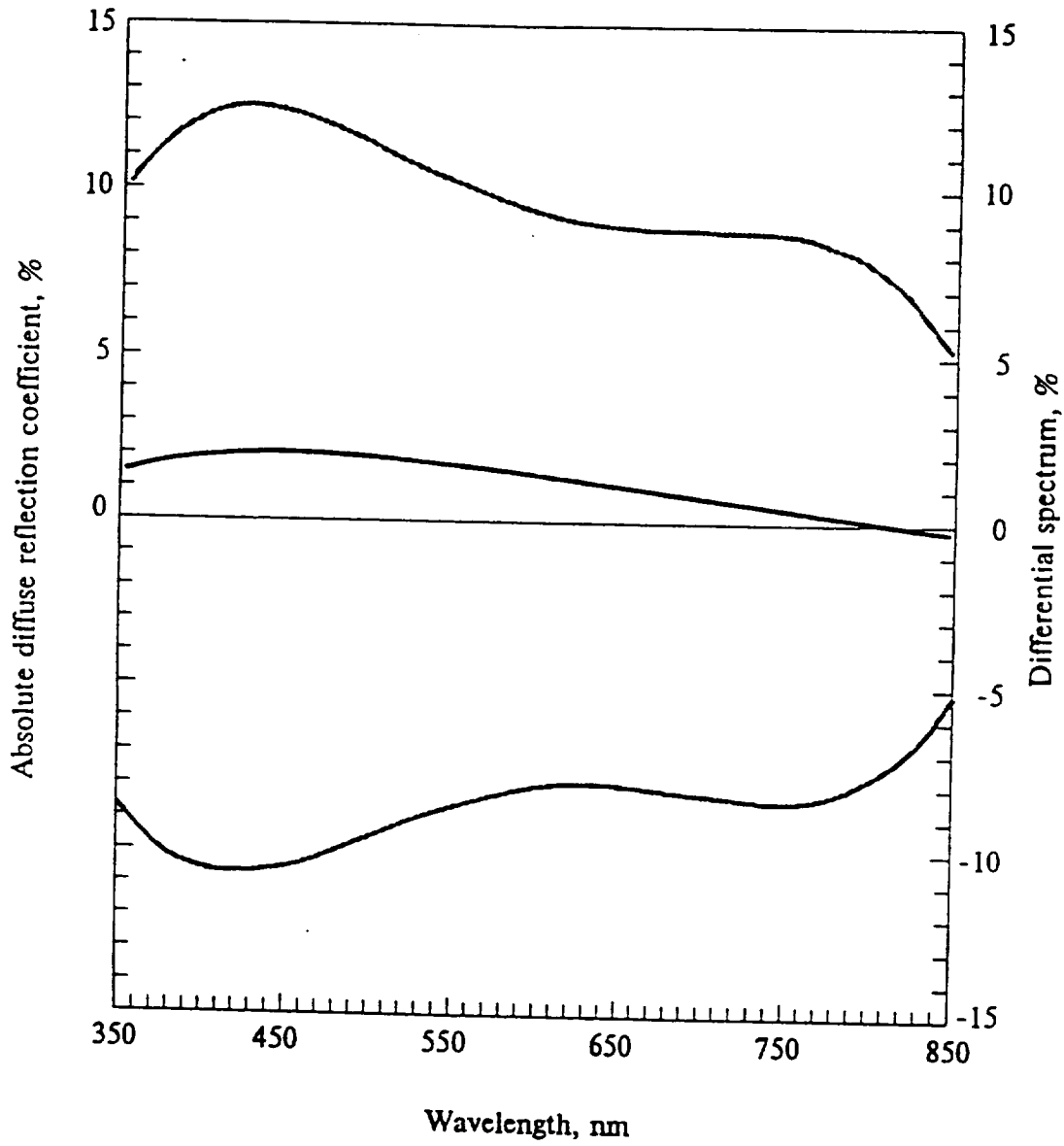


Figure 22. Diffuse UV/visible reflection spectra of the 40-1-12-88 coating.

DIFFUSE REFLECTION SPECTRA  
FOR COATING AK-243 WITHOUT QUARTZ



— before flight  
 — after flight  
 — differential spectrum

Figure 23. Diffuse UV/visible reflection spectra of the unprotected AK-243 coating.

DIFFUSE REFLECTION SPECTRA  
FOR COATING ФП-5246 WITHOUT QUARTZ

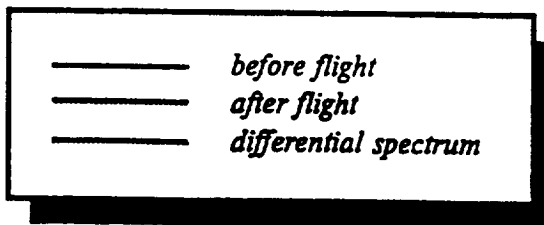
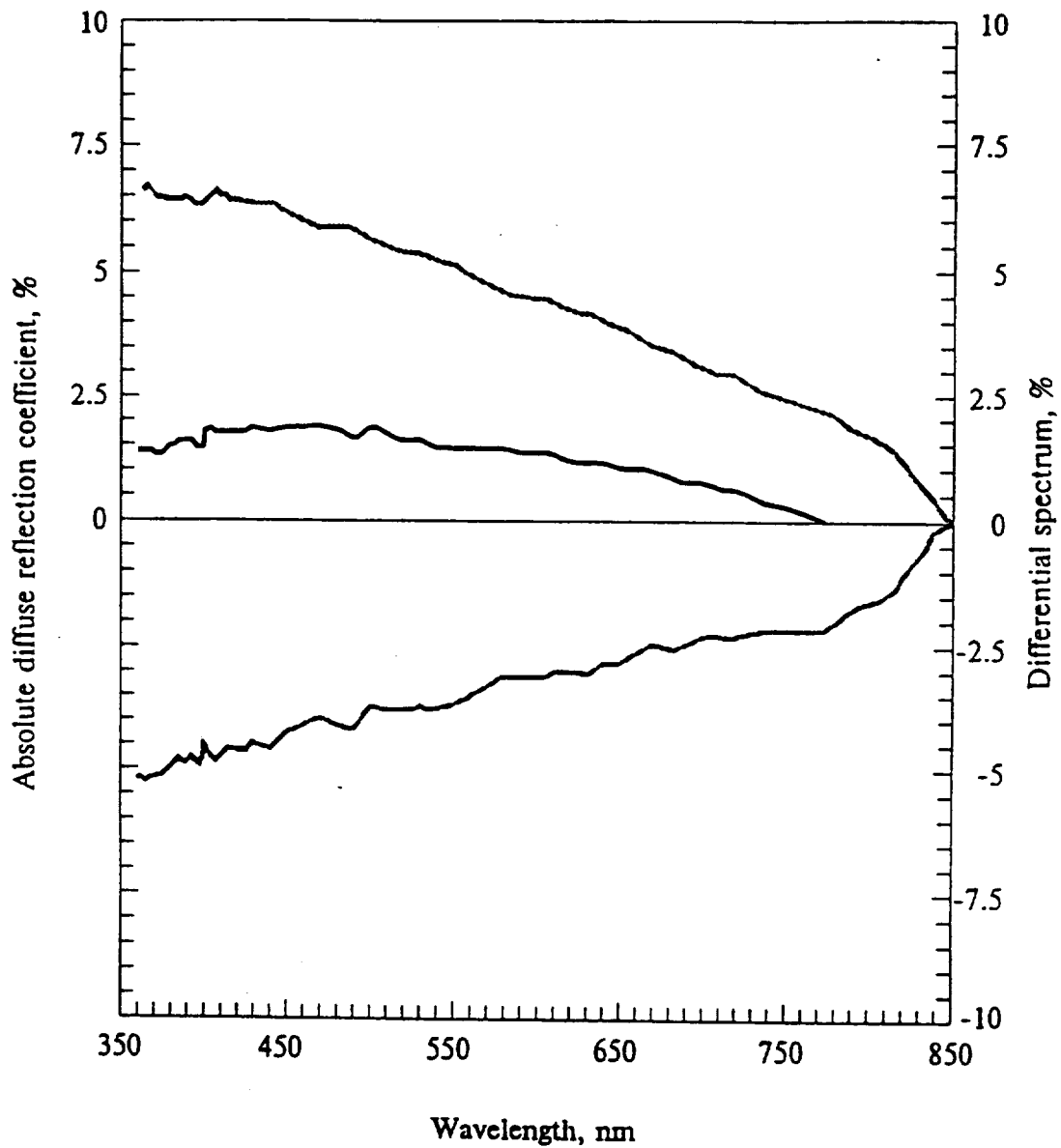


Figure 24. Diffuse UV/visible reflection spectra of the unprotected FP-5246 coating.

DIFFUSE REFLECTION SPECTRA  
FOR COATING AK-243 COVERED BY QUARTZ

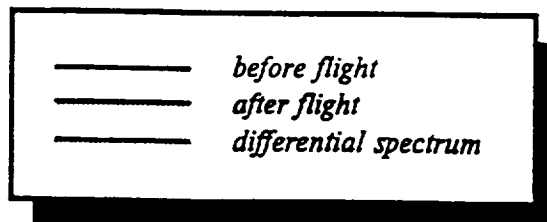
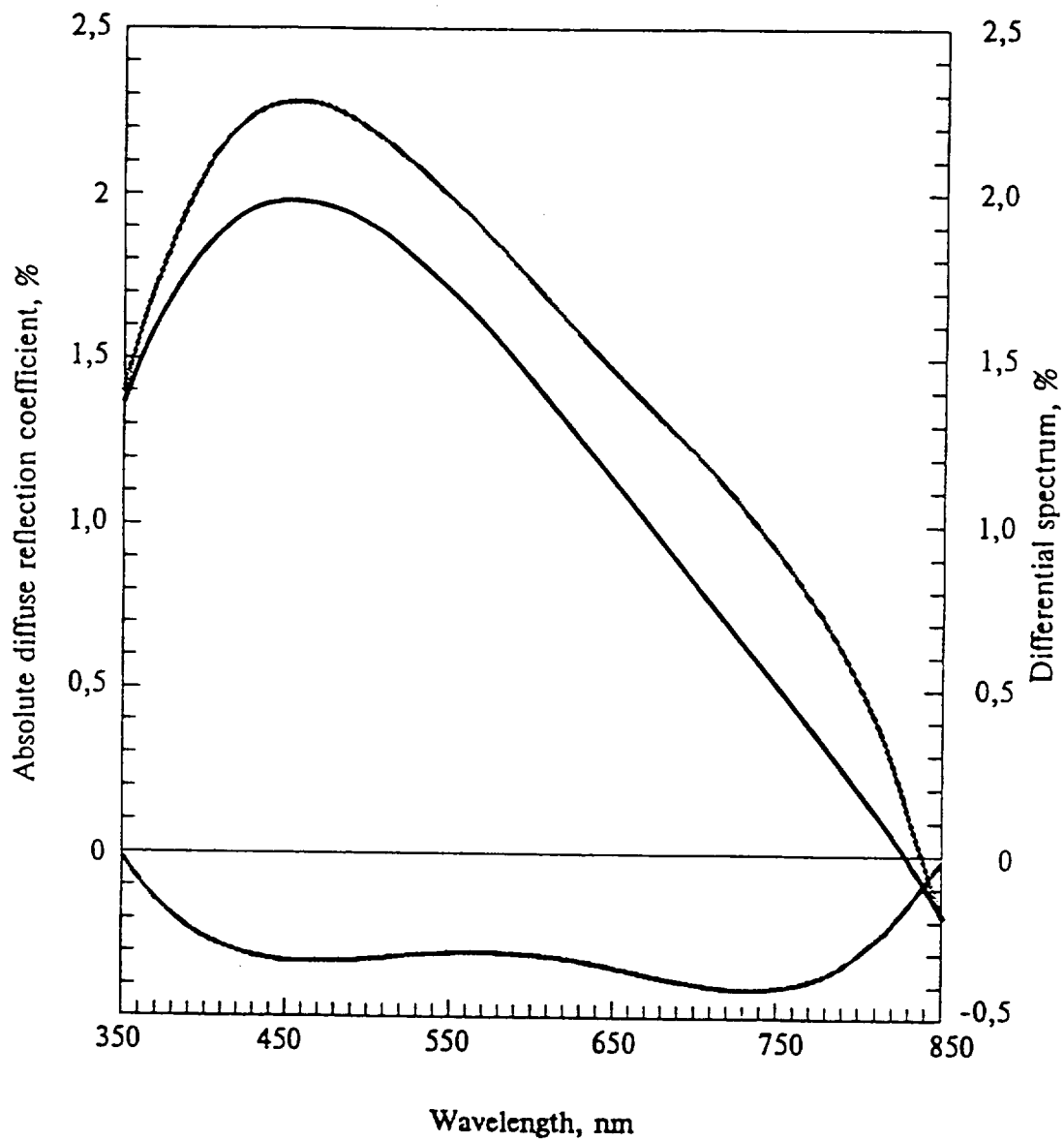
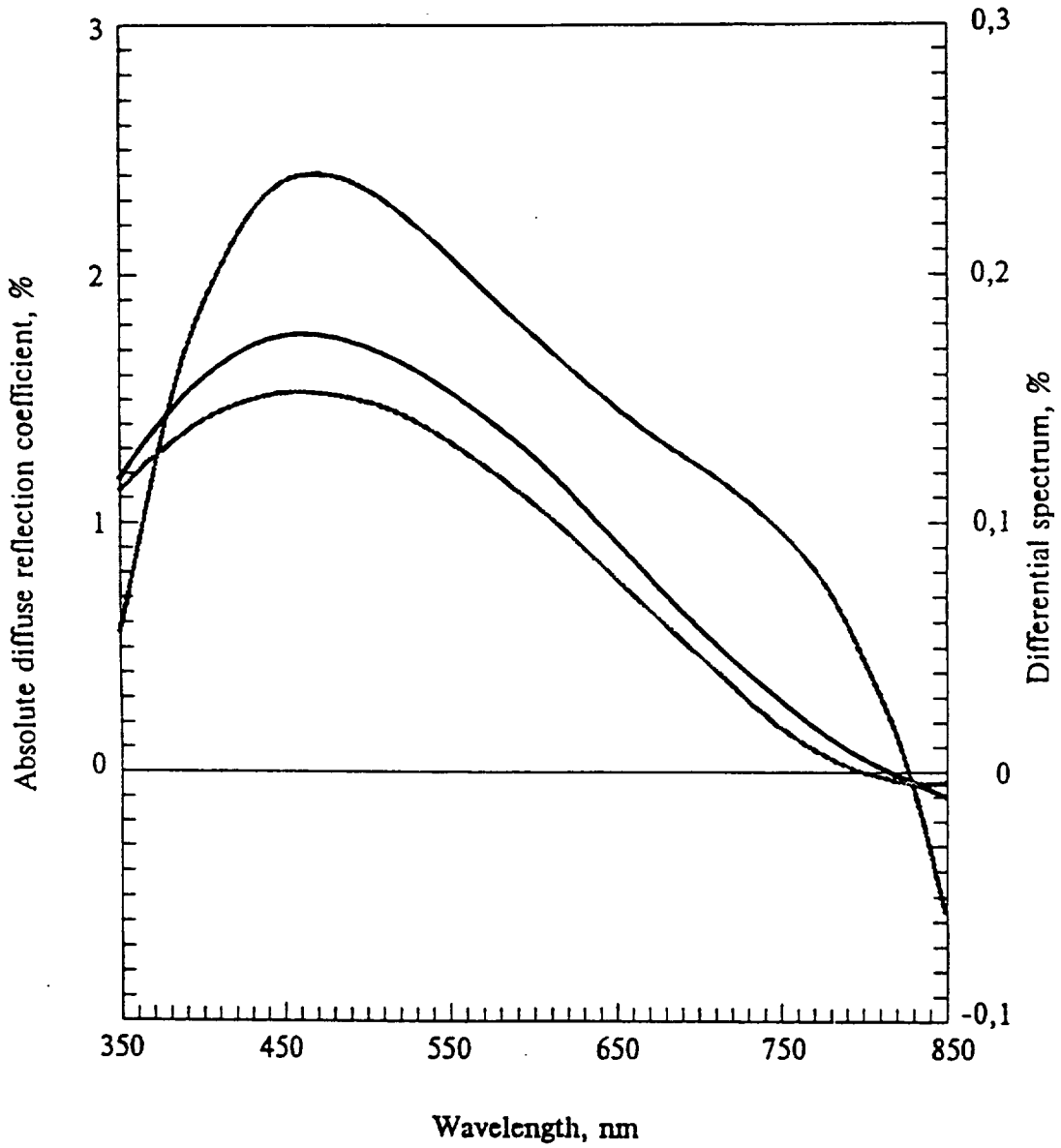


Figure 25. Diffuse UV/visible reflection spectra of the quartz covered AK-243 coating.

DIFFUSE REFLECTION SPECTRA  
FOR COATING ФП-5246 COVERED BY QUARTZ



— before flight  
 — after flight  
 — differential spectrum

Figure 26. Diffuse UV/visible reflection spectra of the quartz covered FP-5246 coating.

DIFFUSE REFLECTION SPECTRA  
FOR COATING AK-512(3)

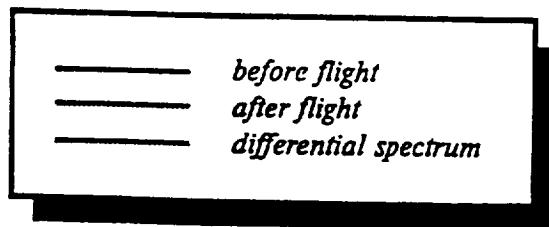
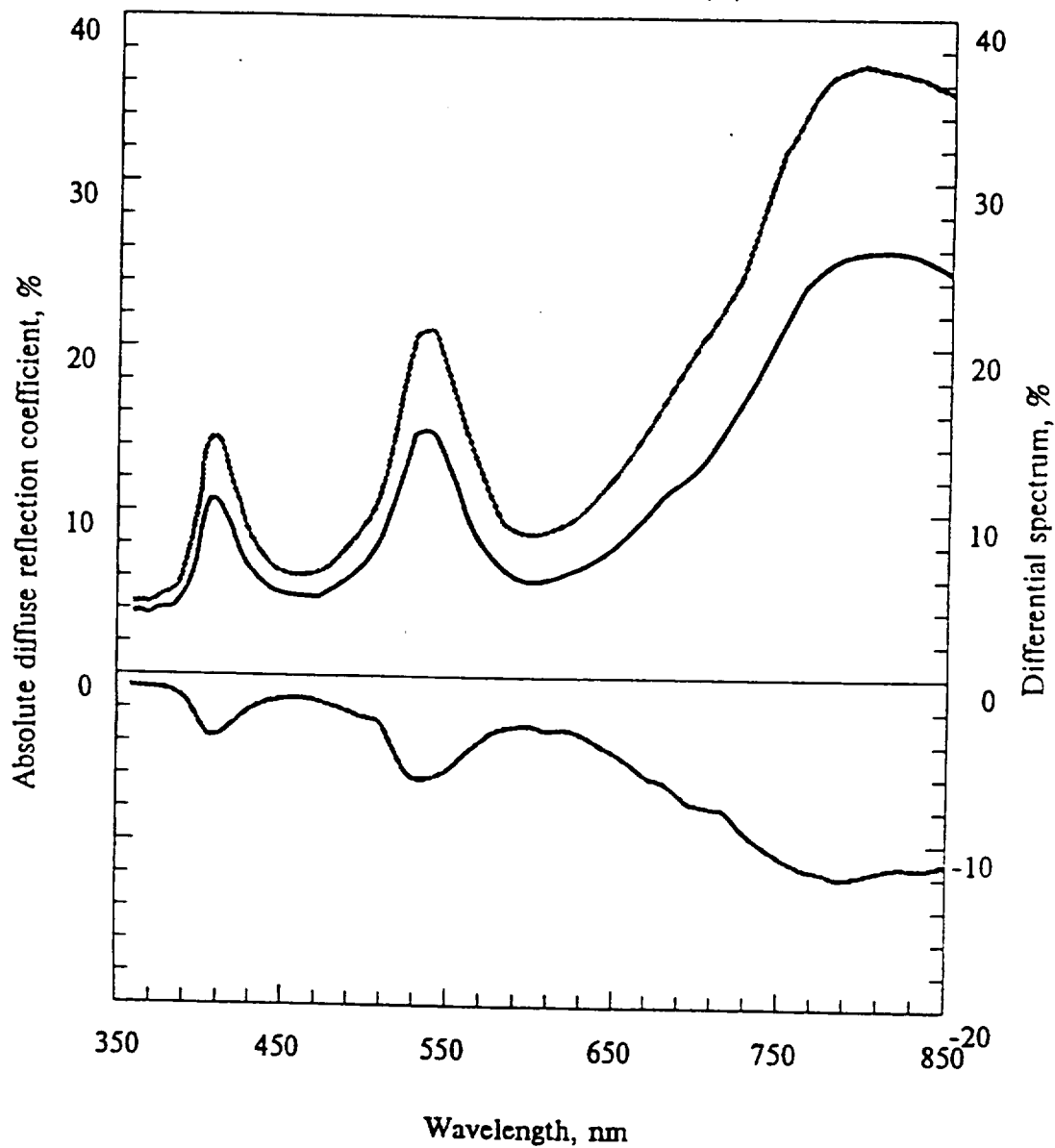


Figure 27. Diffuse UV/visible reflection spectra of the AK-512-g coating.

DIFFUSE REFLECTION SPECTRA  
FOR COATING AK-512

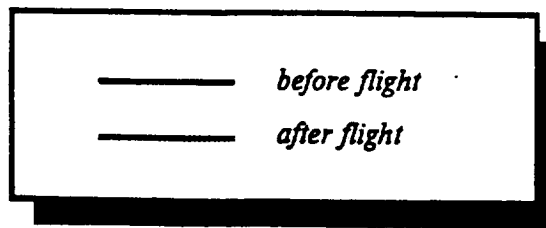
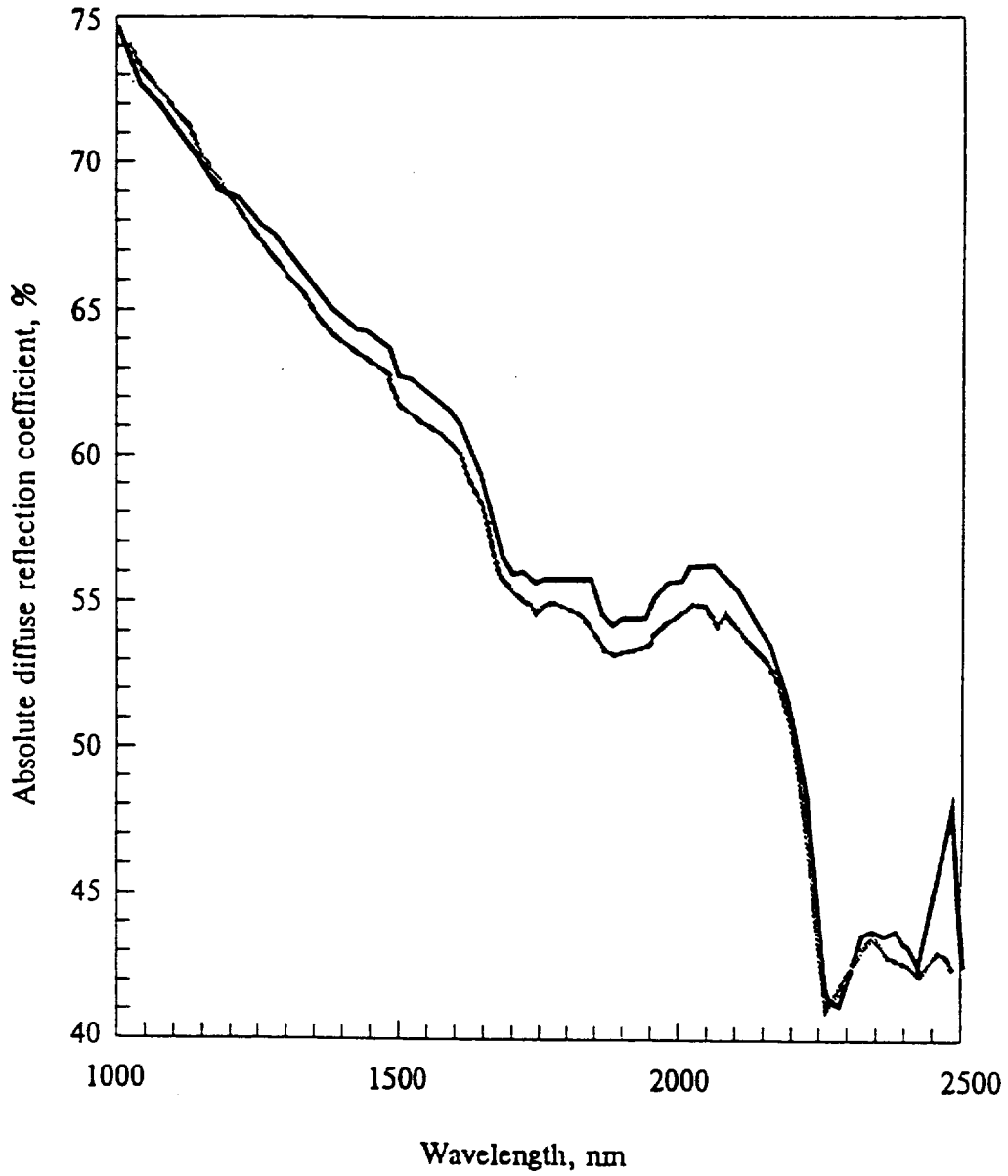


Figure 28. Diffuse IR reflection spectra of the AK-512-w coating.

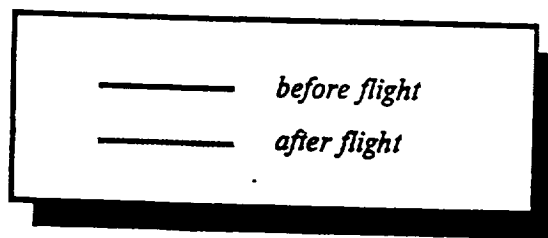
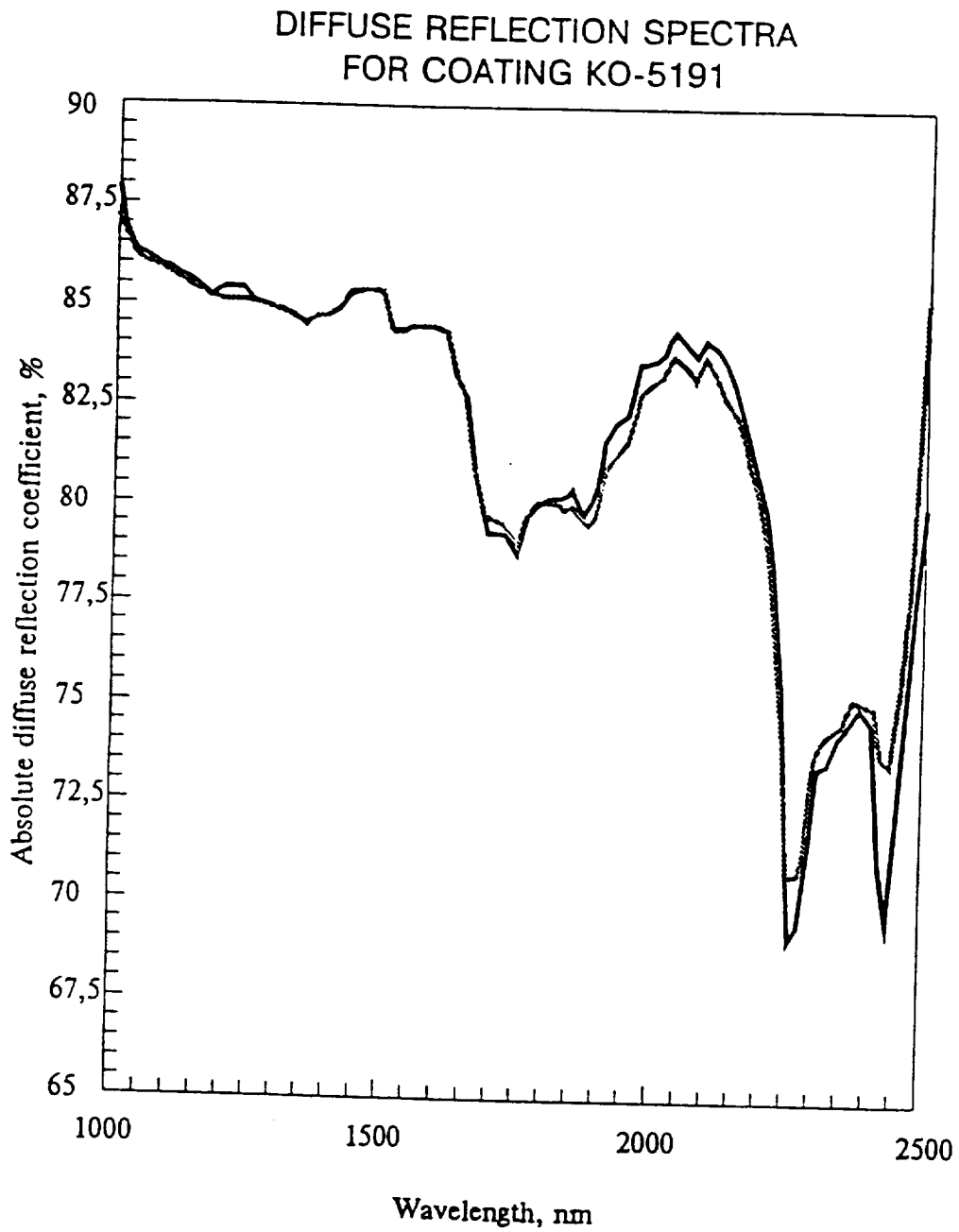


Figure 29. Diffuse IR reflection spectra of the KO-5191 coating.

DIFFUSE REFLECTION SPECTRA  
FOR COATING KO-5258

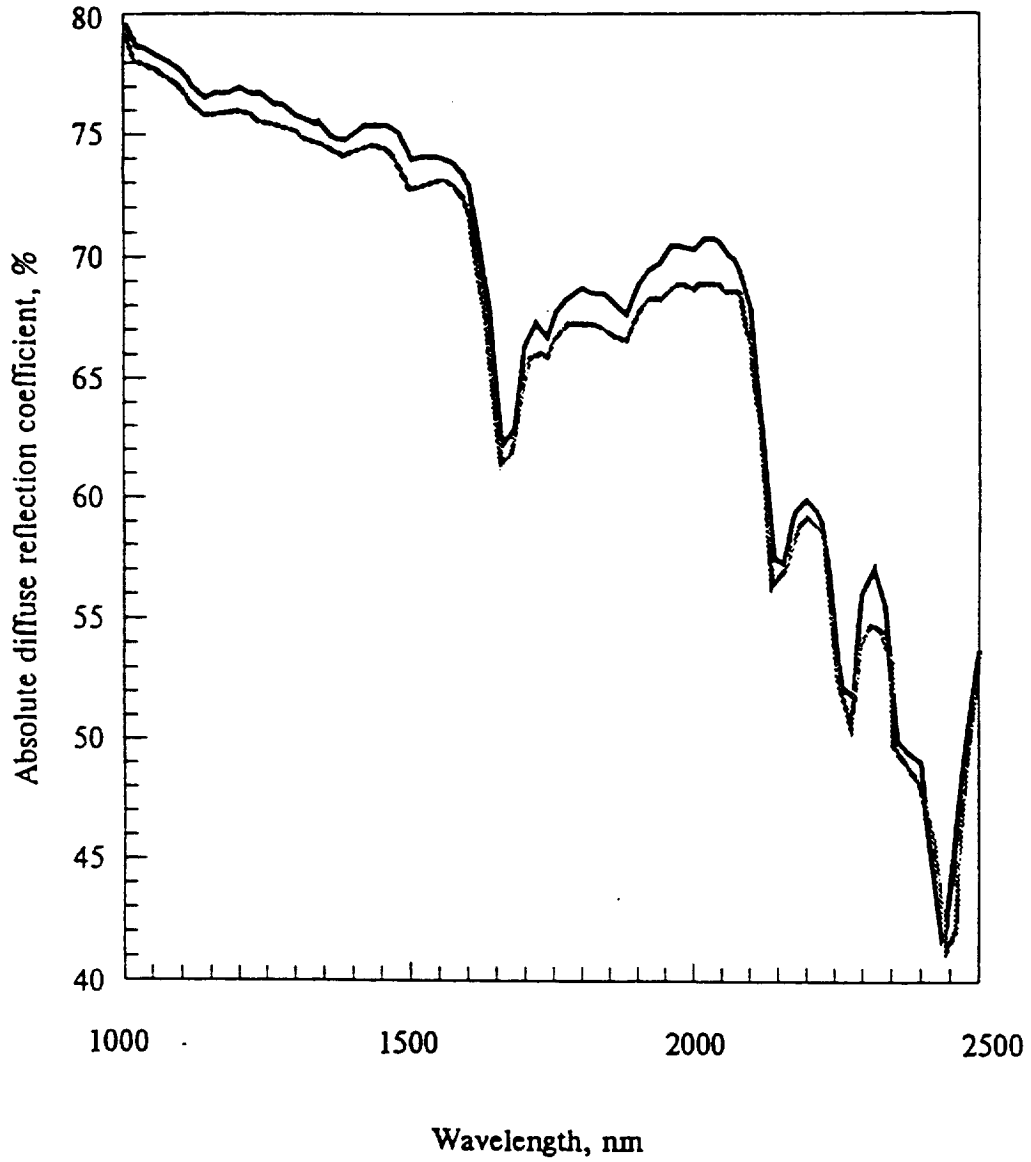
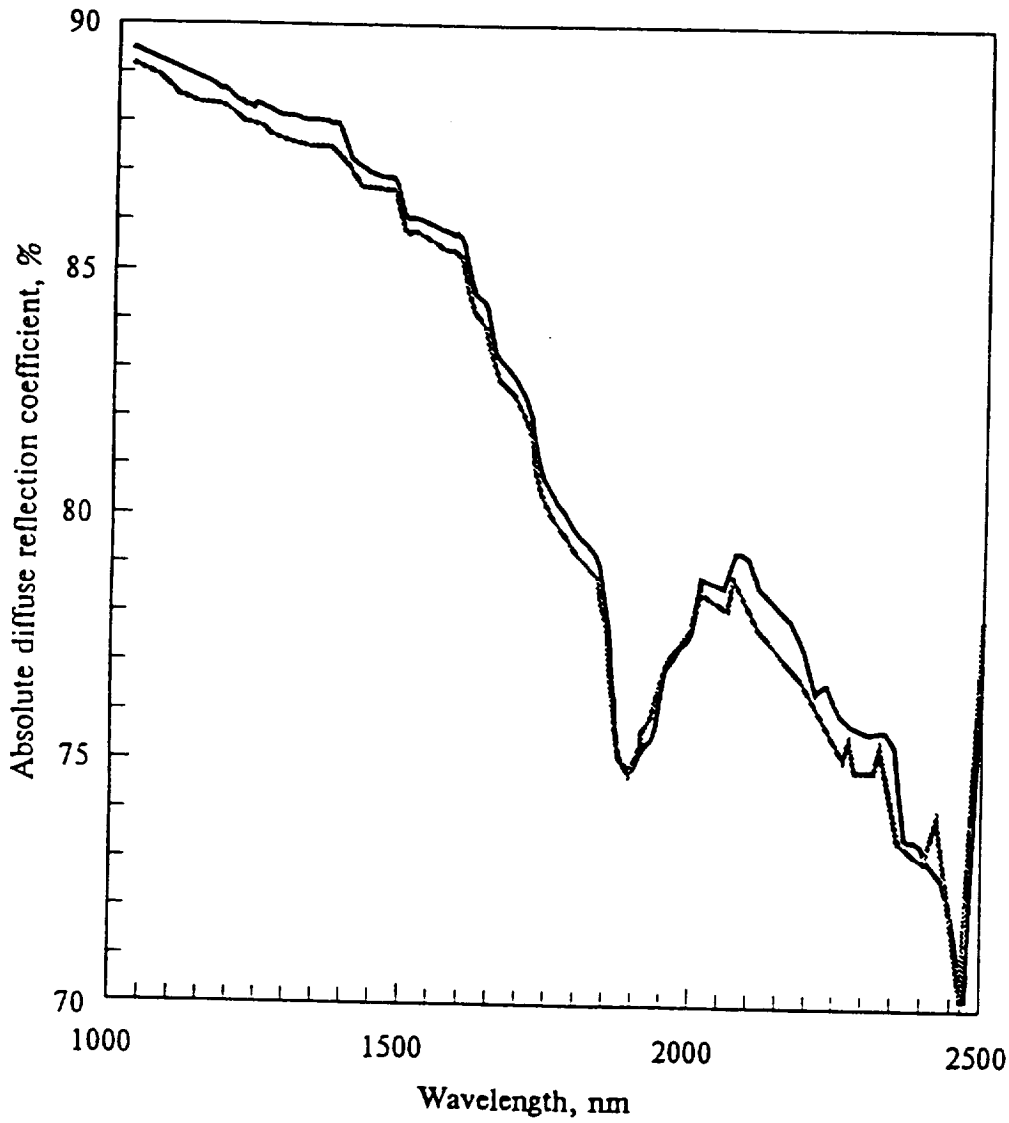


Figure 30. Diffuse IR reflection spectra of the KO-5258 coating.

DIFFUSE REFLECTION SPECTRA  
FOR COATING TP-co-2



— before flight  
— after flight

Figure 31. Diffuse IR reflection spectra for the TP-co-2 coating.

DIFFUSE REFLECTION SPECTRA  
FOR COATING TP-co-10M

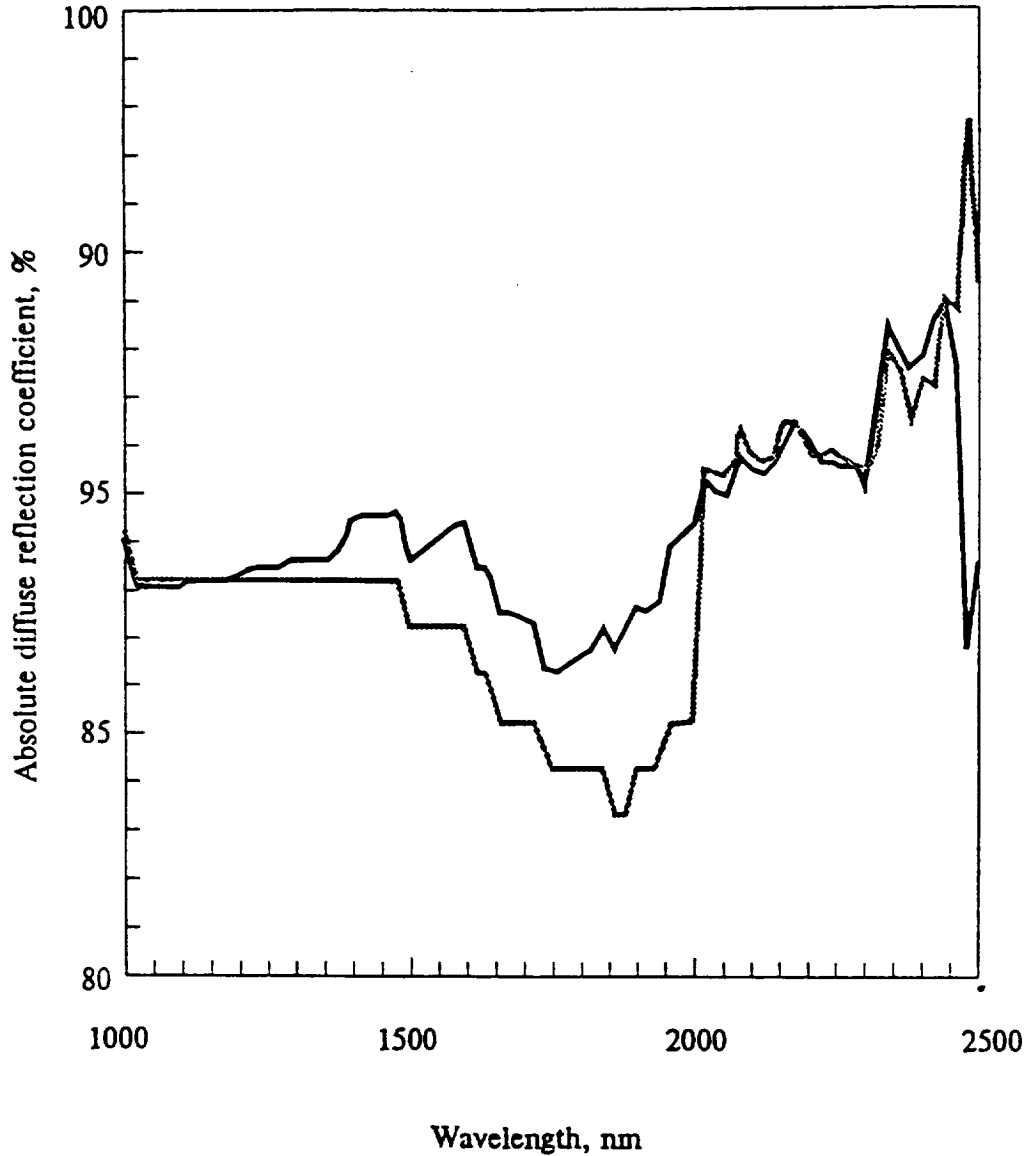
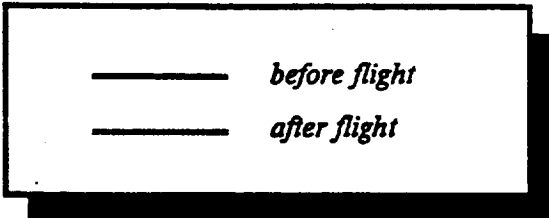


Figure 32. Diffuse IR reflection spectra for the TP-co-10M coating.



DIFFUSE REFLECTION SPECTRA  
FOR COATING TP-co-11

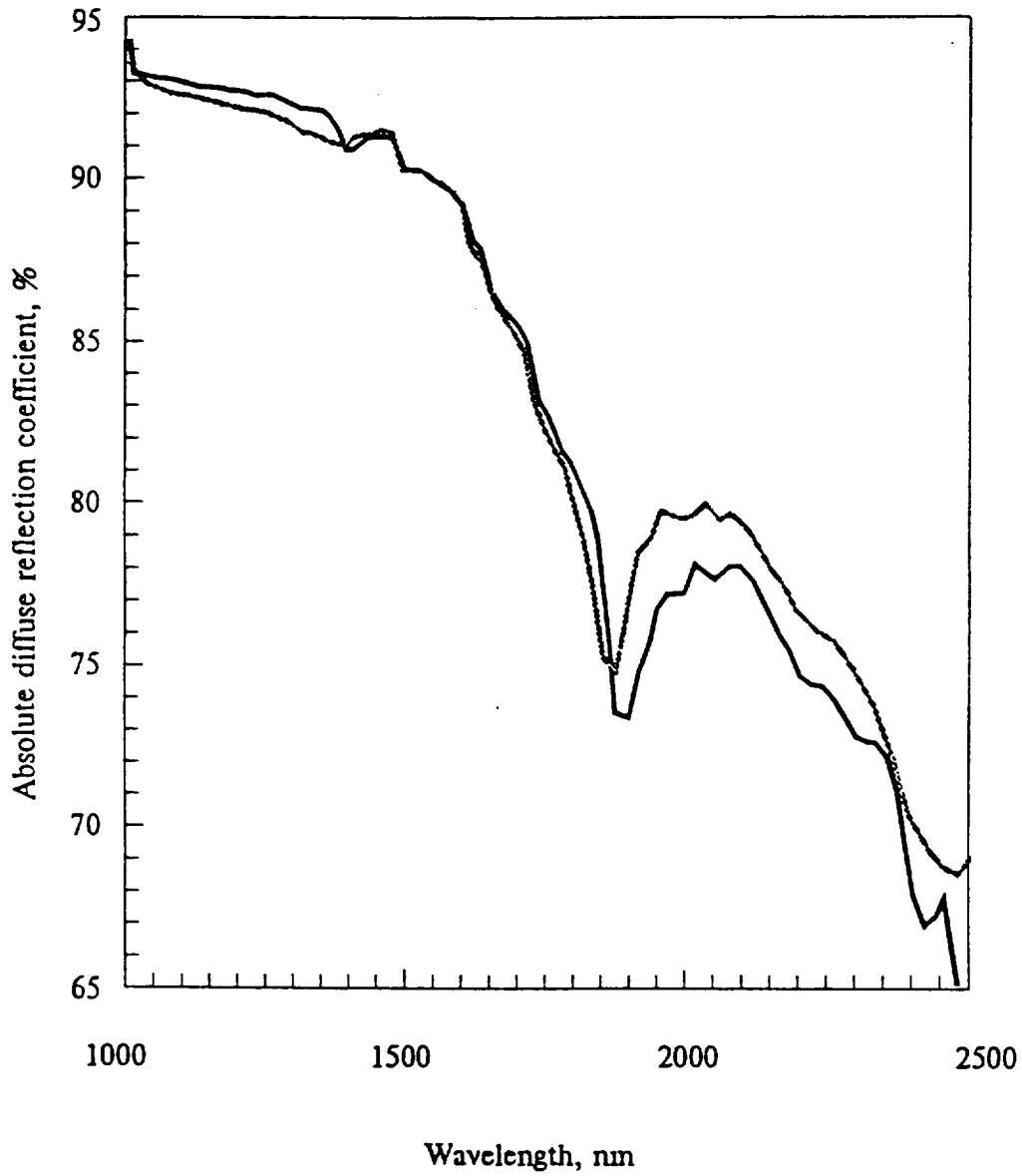
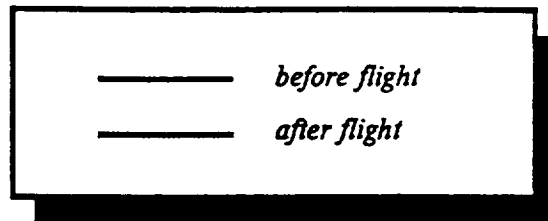


Figure 33. Diffuse IR reflection spectra for the TP-co-11 coating.



DIFFUSE REFLECTION SPECTRA  
FOR COATING TP-co-12

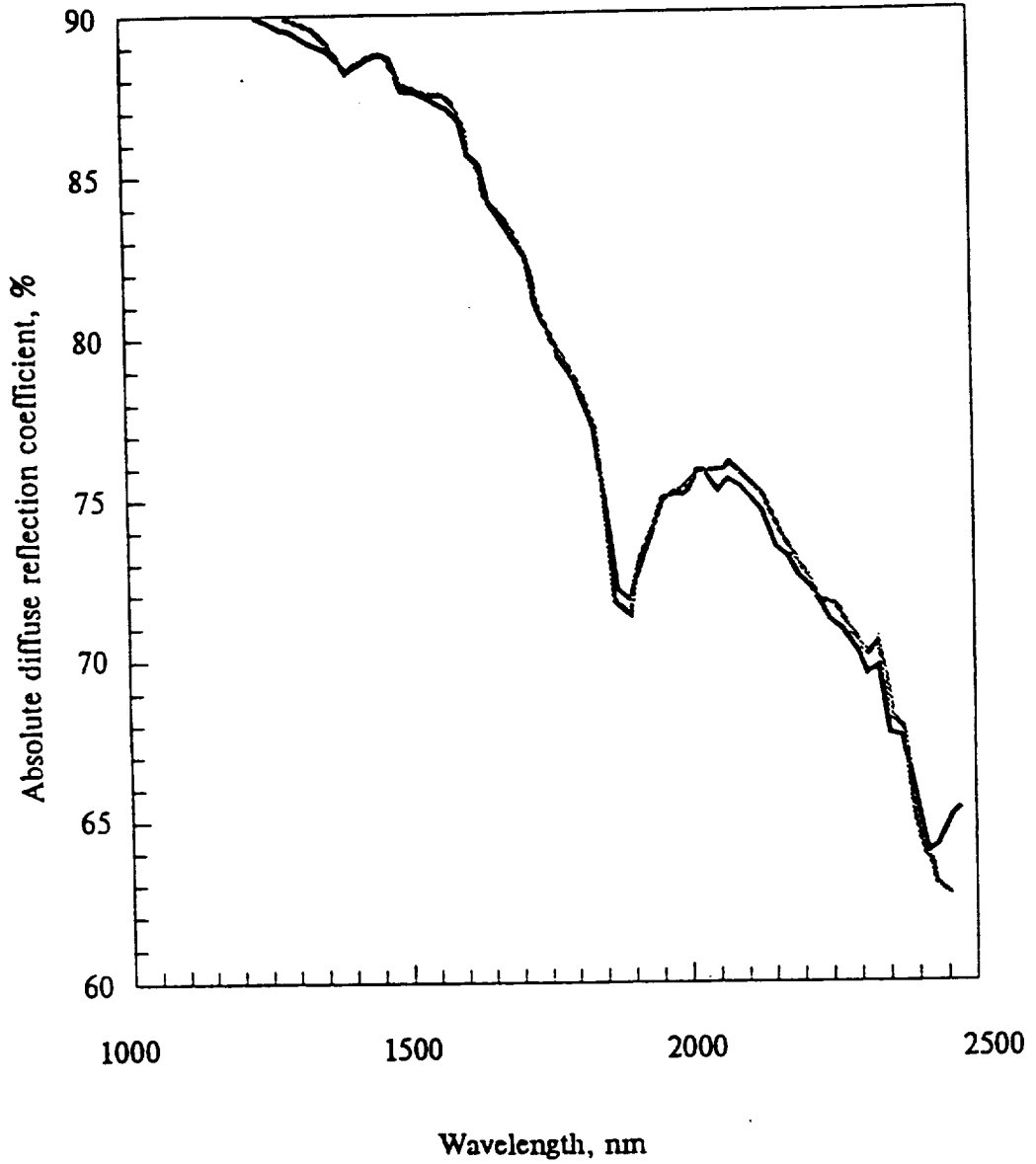
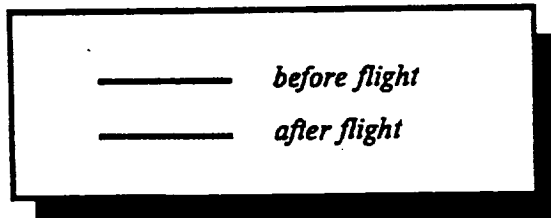


Figure 34. Diffuse IR reflection spectra for the TP-co-12 coating.



DIFFUSE REFLECTION SPECTRA  
FOR COATING TP-co-90

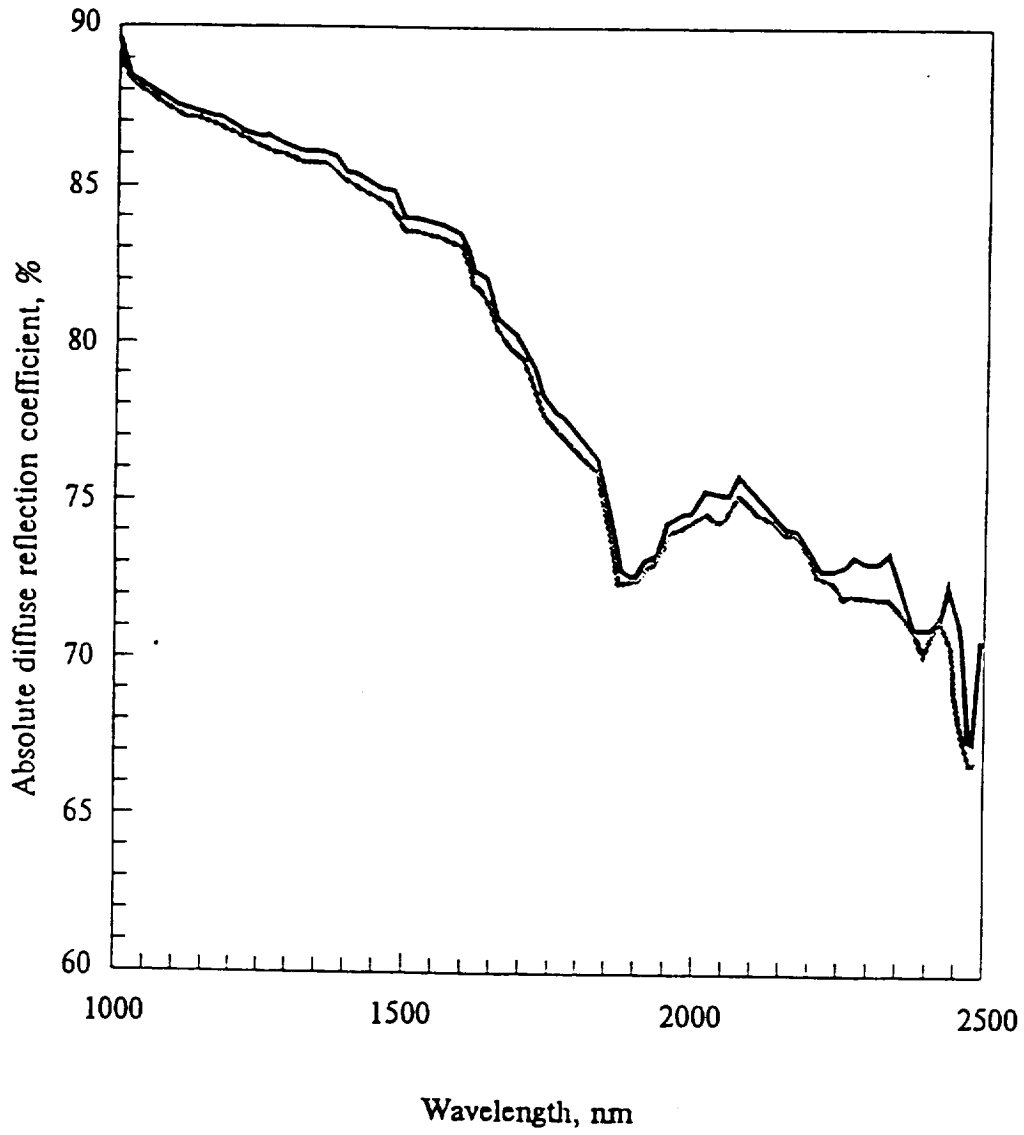
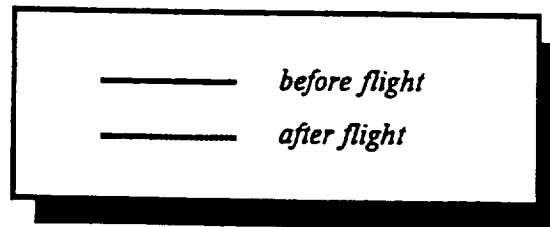
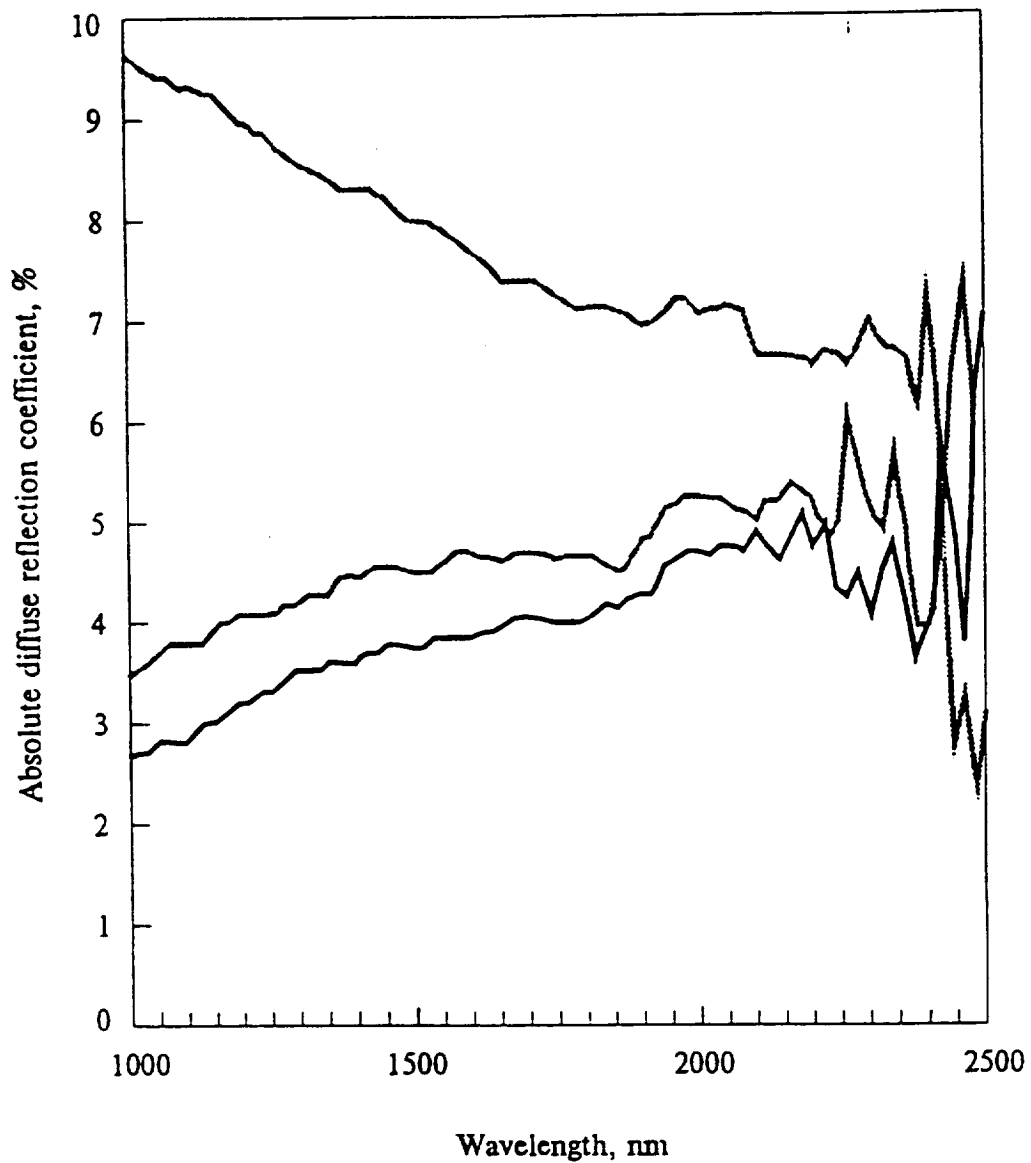


Figure 35. Diffuse IR reflection spectra for the TP-co-90 coating.



# DIFFUSE REFLECTION SPECTRA FOR COATING AK-243



— before flight  
— after flight (without quartz)  
— after flight (covered by quartz)

Figure 36. Diffuse IR reflection spectra for the AK-243 coating.

DIFFUSE REFLECTION SPECTRA  
FOR COATING ФП-5246

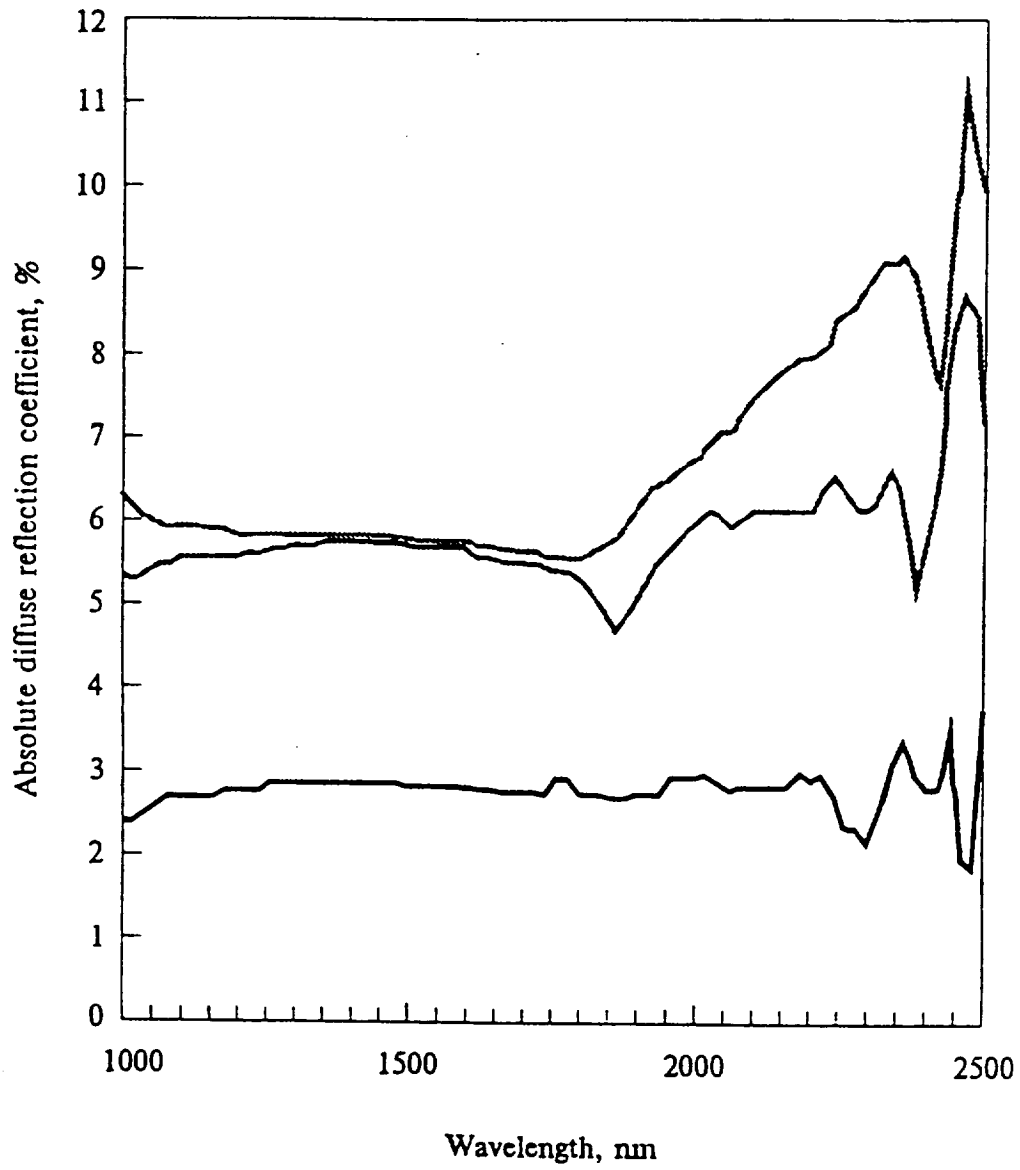
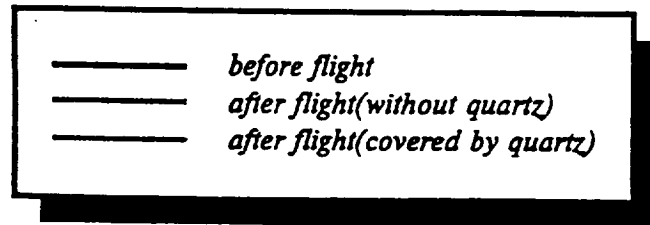


Figure 37. Diffuse IR reflection spectra for the FP-5246 coating.



DIFFUSE REFLECTION SPECTRA  
FOR COATING AK-512(3)

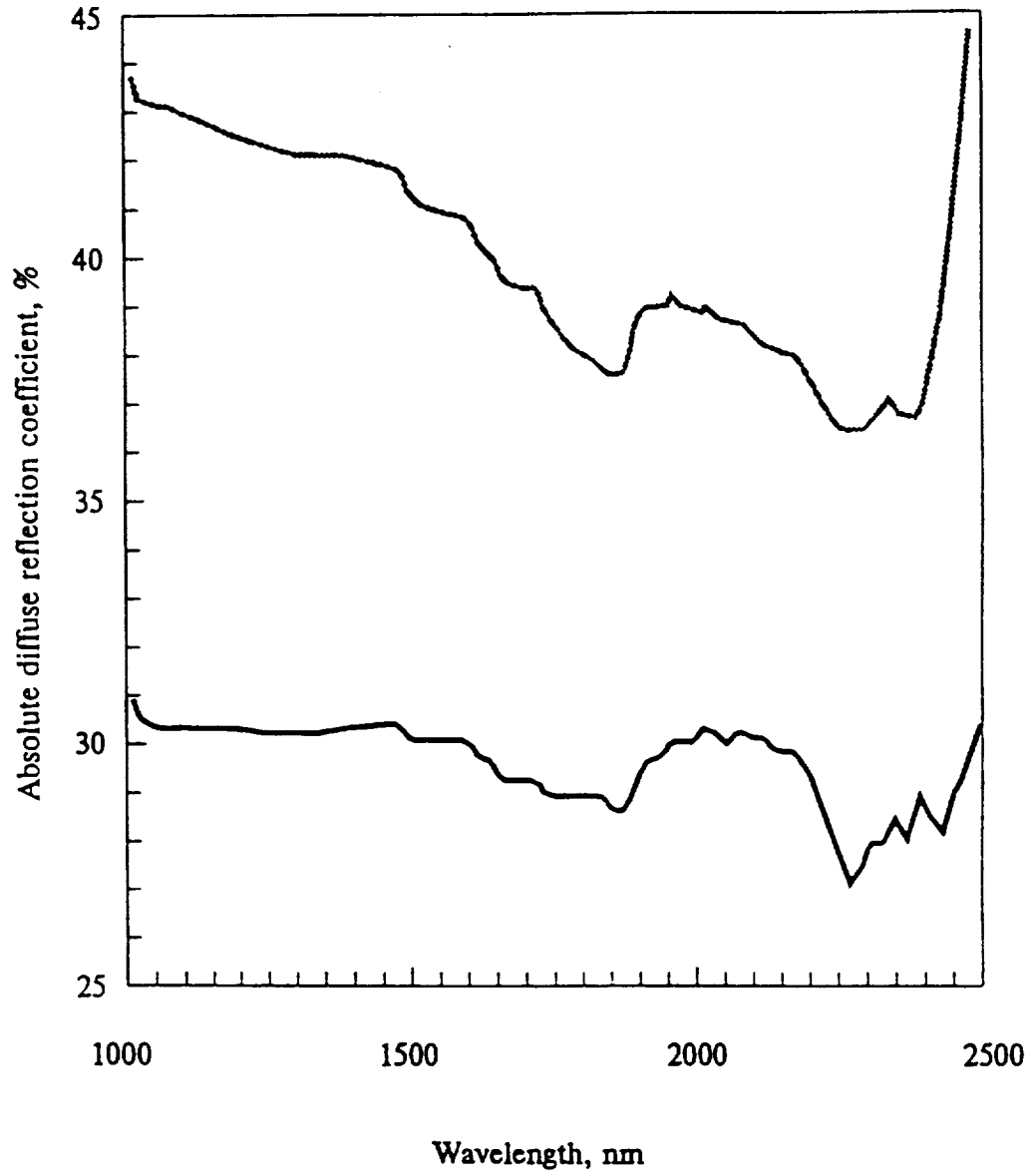
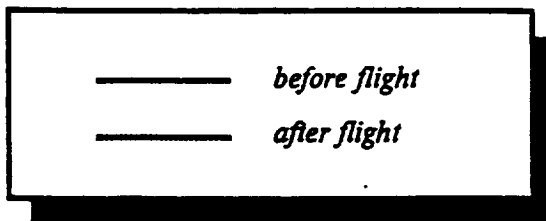


Figure 38. Diffuse IR reflection spectra for the AK-512-g coating.



coating TP-co-12 demonstrated a significant increase of 1.1 mg. It is believed that this increase is due to contamination from the Mir OS condensing on the materials surface when cooled by the Earth's shadow. For coatings which exhibited a mass increase, the contamination deposition effect obviously prevailed over the AO erosion effect.

#### **4.1.5 Chemical Composition Analysis**

The chemical composition analysis data confirms an increase in contamination and a reduction in surface pigment base for all types of materials, Table 11. The white and green AK-512 paints which exhibited a silicon decrease were the only exception. Of particular interest is a comparison of the study results for the black enamels FP-5246 and AK-243. The unprotected FP-5246 sample showed a two-fold increase in silicon content and almost the same decrease in chlorine content. The unprotected AK-243 sample exhibited a decrease of silicon content and a significant increase in molybdenum, which was not present in the coating before the flight. The chemical composition of the protected surfaces varied only moderately, but did exhibit a decrease of silicon content. No changes in the chemical composition of the anodized aluminum coatings were detected.

#### **4.1.6 Conclusions**

- The reflective TP-co-2, TP-co-10M, TP-co-11, and TP-co-12 ZnO and Zn<sub>2</sub>TiO<sub>4</sub> based coatings were the most resistant to space exposure. No changes in the visible or thermo-optical properties, detectable mass loss, or chemical composition were observed.
- The reflective paint coatings 40-1-12-88 and KO-5258 were the least resistance to space exposure. A minor increase in solar absorptance and a decrease of reflection spectra were noticed. The KO-5258 coating showed a more detectable increase in silicon content.
- All absorber coatings were degraded by space environment exposure. These coatings revealed a significant decrease in solar absorptance, an increase in spectral reflection, and significant erosion due to AO. The AK-243 and FP-5246 coatings that were protected by quartz glass did not experience noticeable changes in their characteristics.
- Surface morphology changes were detectable depending on the nature of the TCC. An increase in the number of pores and microcracks were detected, but the sizes of the pigment particles in the coatings showed little variation.

## **4.2 Summary of LDEF Thermal Control Coatings Exposure**

The LDEF Materials Special Investigation Group conducted investigations of a variety of materials on the LDEF, including: aluminum structures, polymers, composites, films, silvered FEP Teflon, and a variety of thermal control coatings.<sup>6-13</sup> Because the Russian RCC-1 experiment was concerned exclusively with TCC, only the LDEF TCC results will be summarized here. A partial list of LDEF TCC materials is provided in Table 12. Because the LDEF contained numerous samples of each material, each of which may have been subjected to a different orbital



environment, it is more appropriate to examine the conclusions for each material separately, before comparing directly with the Russian results. The absorptance and emittance properties of the LDEF TCC, which were measured in accordance with ASTM E 424 and ASTM E 405, are listed in Tables 13 - 14 and 15 - 16, respectively.

#### **4.2.1 White Tedlar**

White Tedlar was expected to show the degrading effects of the Solar UV over the course of the LDEF mission. Instead, the optical properties of this material actually showed slight improvement. The surface remained diffuse and white, apparently as the result of AO erosion breaking loose the degraded surface layers, leaving a clean surface behind.

#### **4.2.2 A276 White Paint**

Chemglaze A276 is a white thermal control paint made with titanium dioxide pigment in a polyurethane binder that has been used on many short term space missions. It was known to degrade moderately under long term UV exposure and to be susceptible to AO erosion. White on black disks of the A276 paint, with and without protective coatings of OI650 and RTV670, were applied to over two hundred tray clamps on the LDEF. Approximately 100 A276 disks were measured for absorptance and emittance making A276 one of the most extensively studied materials on the LDEF.

Protected or trailing edge facing A276 samples underwent a darkening, changing from a white color to tan and eventually dark brown after six years LEO exposure. This is due to a UV degradation of the polyurethane resin portion of the coating that leads to a non-recoverable darkening. The unprotected samples remained very white. Apparently, as the exposed A276 surfaces degraded they were also eroded by AO, leaving a fresh, undamaged surface, Figure 39. The AO eroded the polyurethane portion of the paint, leaving behind paint pigment particles. The total erosion depth was measured and found to be on the order of 10 microns. Pre-flight, in space, and post-flight measurements of solar absorptance indicate that both protective coatings prevented AO erosion but allowed the solar UV to degrade the A276. Unprotected A276 samples show only small amounts of degradation. The overcoated samples indicated cracking and peeling post-flight, while the unprotected samples remained smooth.

#### **4.2.3 Z93 White Paint**

Z93 is a white thermal control paint made with zinc oxide pigment in a potassium silicate binder. Most Z93 samples were almost impervious to the 69 months of LEO exposure making it a leading candidate for Space Station applications. The Z93 samples showed an initial improvement in solar absorptance due to an increased reflectance above 1300 nm, Figure 40. This is offset by a very slow degradation below 1000 nm which results in an overall degradation of 0.01 in solar absorptance.

Table 12. A partial list of thermal control coating materials on the LDEF.

Material		
Class	Reference	Chemical Nature
Reflector	White Tedlar	TiO <sub>2</sub> / polyurethane ZnO / silicone Zn <sub>2</sub> TiO <sub>4</sub> / silicone ZnO / K silicate
	A276	
	Z93	
	S13GLO	
	YB71	
	Silver Teflon	
Absorber	D111	carbon / polyurethane TiO <sub>2</sub> + C / polyurethane
	Z302	
	Z306	
Other	Chromic Acid Anodized Al	-

Table 14. Solar absorptance values for LDEF thermal control coatings - thermal control surfaces experiment.

Materials	Solar Absorptance		
	Pre-Flight	Post-Flight	$\Delta\alpha$
Tedlar	-	-	-
A276	0.25	0.24	-0.01
w/RTV670	0.27	0.62	0.35
w/OI650	0.25	0.59	0.34
Z93	0.14	0.15	0.01
S13GLO	0.18	0.37	0.19
YB71	0.13	0.15	0.02
Silver Teflon	0.06	0.08	0.02
D111	0.98	0.99	0.01
Z302	0.97	0.98	0.01
w/RTV670	0.98	0.99	0.01
w/OI650	0.98	0.99	0.01
Cr Anodize	0.40	0.47	0.07
Position - Row 9, Angle off Ram - 8.1°, AO Fluence - $8.99 \times 10^{21}$ atoms cm <sup>-2</sup> , Sun Hours - 11,200			

Table 16. Emittance values for LDEF thermal control coatings - thermal control surfaces experiment.

Materials	Emittance		
	Pre-Flight	Post-Flight	$\Delta\alpha$
Tedlar	-	-	-
A276	0.90	0.93	0.03
w/RTV670	0.91	0.88	-0.03
w/OI650	0.90	0.89	-0.01
Z93	0.91	0.92	0.01
S13GLO	0.90	0.89	-0.01
YB71	0.90	0.89	-0.01
Silver Teflon	0.81	0.78	-0.03
D111	0.93	0.90	-0.03
Z302	0.91	0.92	0.01
w/RTV670	0.91	0.90	-0.01
w/OI650	0.90	0.90	0.00
Cr Anodize	0.84	0.78	-0.03
Position - Row 9, Angle off Ram - 8.1°, AO Fluence - $8.99 \times 10^{21}$ atoms cm <sup>-2</sup> , Sun Hours - 11,200			

#### 4.2.4 S13GLO White Paint

S13G and its low outgassing version, S13GLO, are white thermal control paints made with zinc oxide pigment in a RTV602 silicone binder. The S13G and S13GLO samples were predicted to degrade moderately in the Solar UV environment. Historically, this instability has been attributed to the formation of an easily bleachable (by oxygen) infrared absorption band between ~ 700 and 2800 nm. This degradation is often not observed by post-flight reflectance measurements performed in air because exposure to the atmosphere can result in rapid and complete recovery of the UV-induced damage. To prevent the bleaching the zinc oxide pigment particles are encapsulated in potassium silicate to provide greater UV stability. There is, however, additional degradation of the

Table 13. Solar absorptance values for LDEF thermal control coating materials - atomic oxygen stimulated outgassing experiment.

Material		Solar Absorptance									
		Leading Edge					Trailing Edge				
		Control	Open	$\Delta\alpha$	UV Only	Control	Open	$\Delta\alpha$	UV Only		
Reflector	A276	0.21	0.20	-0.01	0.35	0.18	0.18	0.26	+0.08	0.20	
	S13G	0.17	0.17	-	0.18	0.17	0.17	0.28	+0.11	0.21	
	S13GLO	0.18	0.19	+0.01	0.19	0.16	0.19	0.19	0.03	0.19	
	YB71	0.16	0.17	+0.01	0.19	0.16	0.16	0.17	0.01	0.16	
	Z93	0.16	0.17	+0.01	0.17	0.16	0.17	0.17	0.01	0.16	
Absorber	Z306	0.95	0.96	+0.01	0.95						
Leading Edge: Position - C9, Angle off Ram - 8.1°, AO Fluence - $8.99 \times 10^{21}$ atoms $\text{cm}^{-2}$ , Sun Hours - 11,200											
Trailing Edge: Position - C9, Angle off Ram - 171.9°, AO Fluence - $1.32 \times 10^{17}$ atoms $\text{cm}^{-2}$ , Sun Hours - 11,100											

Table 15. Emittance values for LDEF thermal control coating materials - atomic oxygen stimulated outgassing experiment.

Material		Emittance									
		Leading Edge					Trailing Edge				
		Control	Open	$\Delta\alpha$	UV Only	Control	Open	$\Delta\alpha$	UV Only		
Reflector	A276	0.87	0.92	+0.05	0.97	0.90	0.90	0.89	-0.01	0.90	
	S13G	0.90	0.88	-0.02	0.90	0.89	0.89	0.91	+0.02	0.89	
	S13GLO	0.89	0.98	+0.09	0.89	0.89	0.89	0.89	-	0.89	
	YB71	0.89	0.89	-	0.93	0.89	0.89	0.90	-0.01	0.89	
	Z93	0.91	0.92	+0.01	0.93	0.91	0.91	0.90	-0.01	0.91	
Absorber	Z306	0.84	0.80	-0.04	0.80						
Leading Edge: Position - C9, Angle off Ram - 8.1°, AO Fluence - $8.99 \times 10^{21}$ atoms $\text{cm}^{-2}$ , Sun Hours - 11,200											
Trailing Edge: Position - C9, Angle off Ram - 171.9°, AO Fluence - $1.32 \times 10^{17}$ atoms $\text{cm}^{-2}$ , Sun Hours - 11,100											

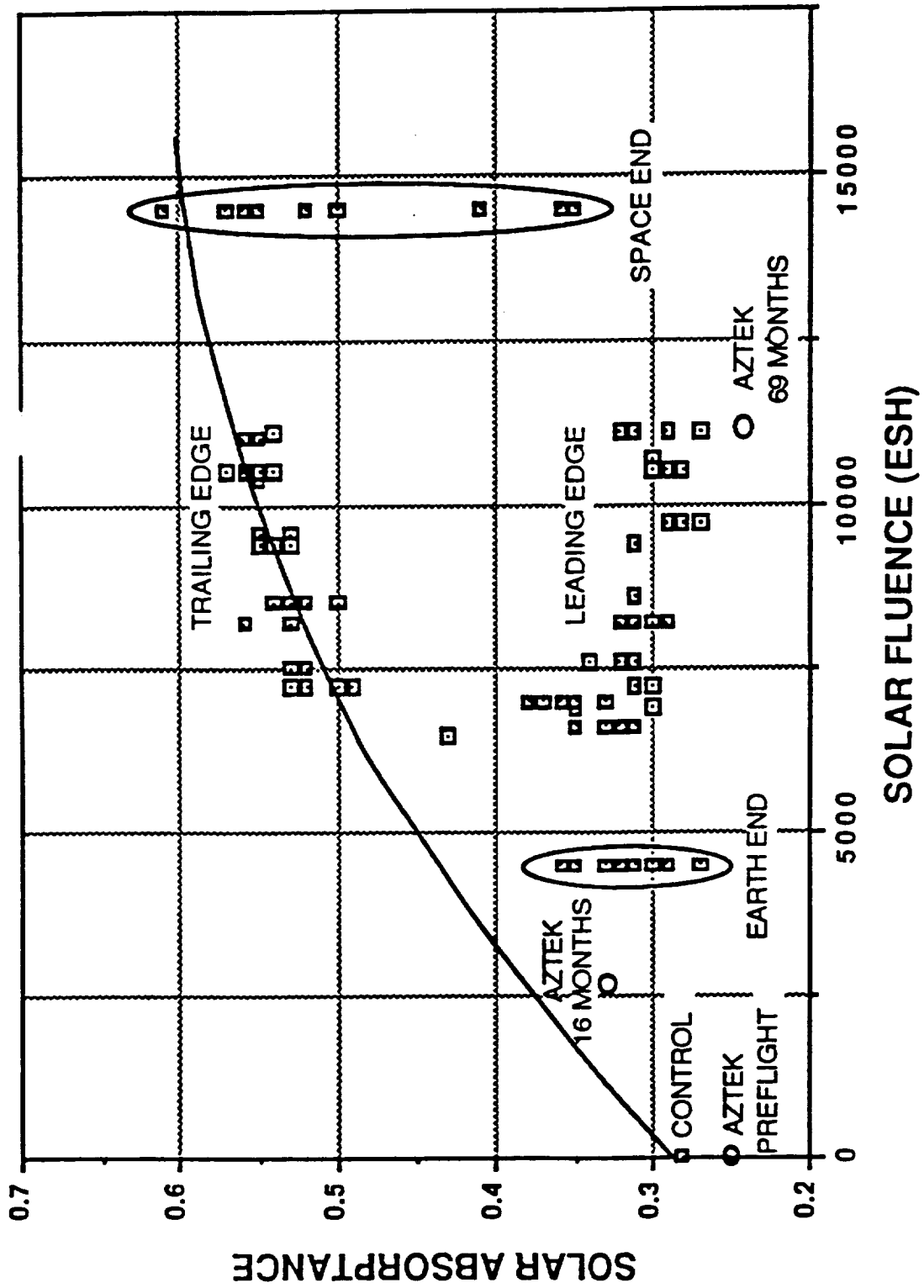


Figure 39: Solar absorbance vs solar UV exposure for A276 white thermal control paint.

# Z93 White Paint - Sample C95 69.2 Months Exposure

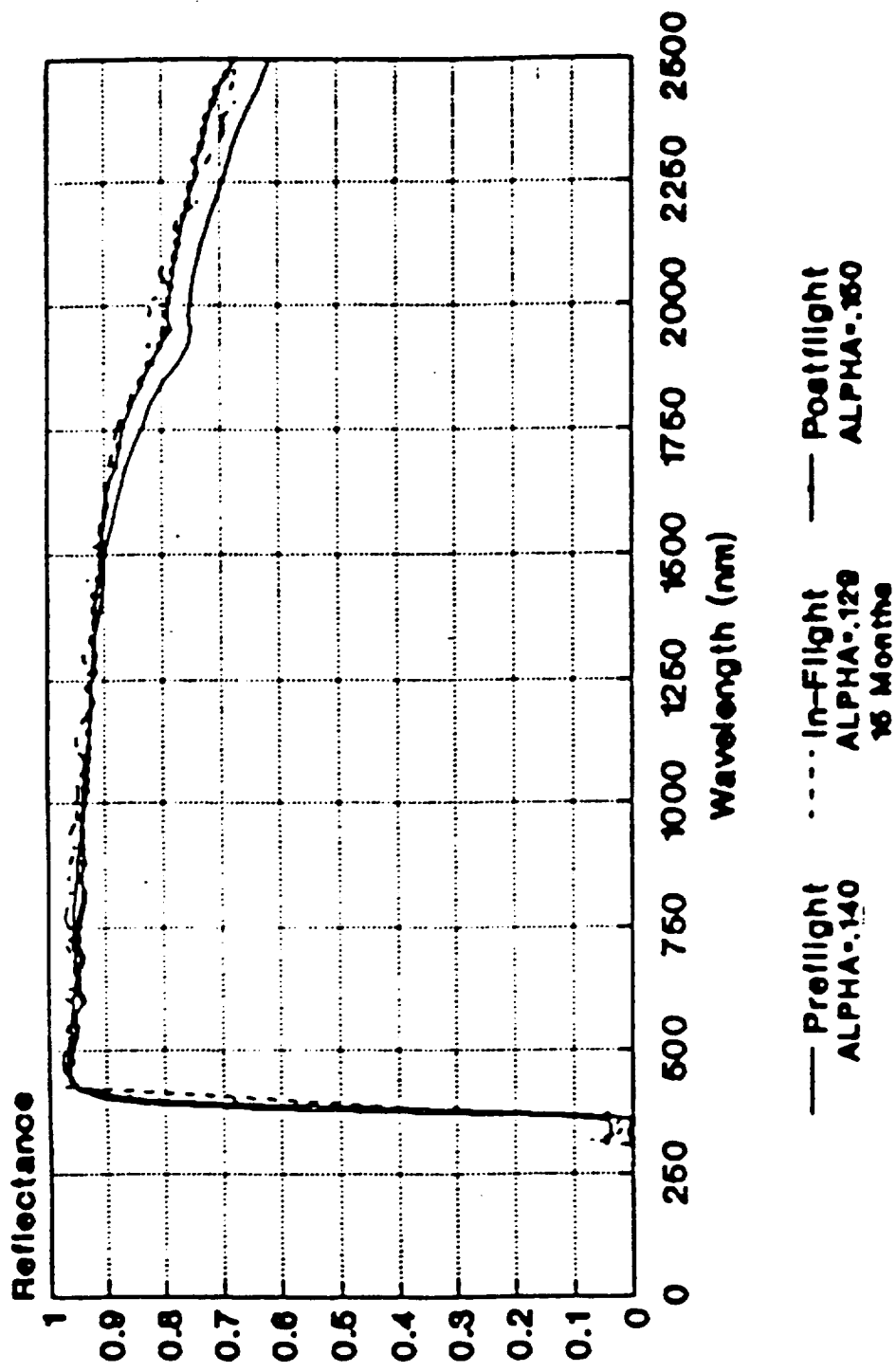


Figure 40. Diffuse solar reflectance for Z93 white thermal control paint.

silicone binder that only partially recovers upon exposure to the atmosphere. Both leading and trailing edge samples of S13GLO were observed to degrade significantly during the LDEF mission, Table 17. Unlike the A276 however, there is little difference in the surface morphologies between leading and trailing edge samples. Note that these tests were conducted on the early 1980's version of S13GLO. RTV602 has since been discontinued and the silicone used in the currently produced material has a slightly different formulation. More recent test results may vary from these flight data.

**Table 17. Post-flight analysis of LDEF thermal control coating samples.**

Sample	Row	$\alpha_s$	Comment
S13G	Control	0.213	-
	L3	0.266	discolored, rough
	T3	0.475	discolored, rough
	L6	0.233	discolored, rough
	T6	0.238	discolored, rough
Silver Teflon	Control	0.109	-
	L3	0.126	bright, hazy, pitted
	T3	0.177	bright, hazy, scuffed
	L6	0.135	bright, hazy, tarnish
	T6	-	-
D111	Control	0.975	-
	L3	0.979	nonreflective, pitted
	T3	0.982	nonreflective,
	L6	0.981	chipped
	T6	-	particulates
			-

#### 4.2.5 YB71 White Paint

YB71 is a white thermal control paint made from zinc orthotitanate. The YB71 coatings behaved similarly to the Z93 samples. A small increase in infrared reflectance early in the mission caused a decrease in solar absorptance, Figure 41. This was followed by a slow, long term degradation resulting in a small overall increase in solar absorptance. Samples with YB71 applied over a primer coat of Z93 had a somewhat lower absorptance than did other YB71 samples.

#### 4.2.6 Silver Teflon

There were a variety of silver Teflon materials flown on the LDEF. The Thermal Control Surfaces Experiment (TCSE) flew one 2 mil thick silver FEP Teflon sample, and two 5 mil thick, (specular and diffuse), samples. The exterior surfaces underwent significant appearance changes where the surface color was changed to a diffuse, whitish appearance due to AO erosion. Although the visual appearance was noticeably changed, the solar absorptance of the 5 mil samples did not degrade significantly and there was little change in emittance. The 2 mil sample had developed a brown discoloration, under the Teflon surface, and more than doubled the solar

**YB71 over Z93 - Sample C93  
69.2 Months Exposure**

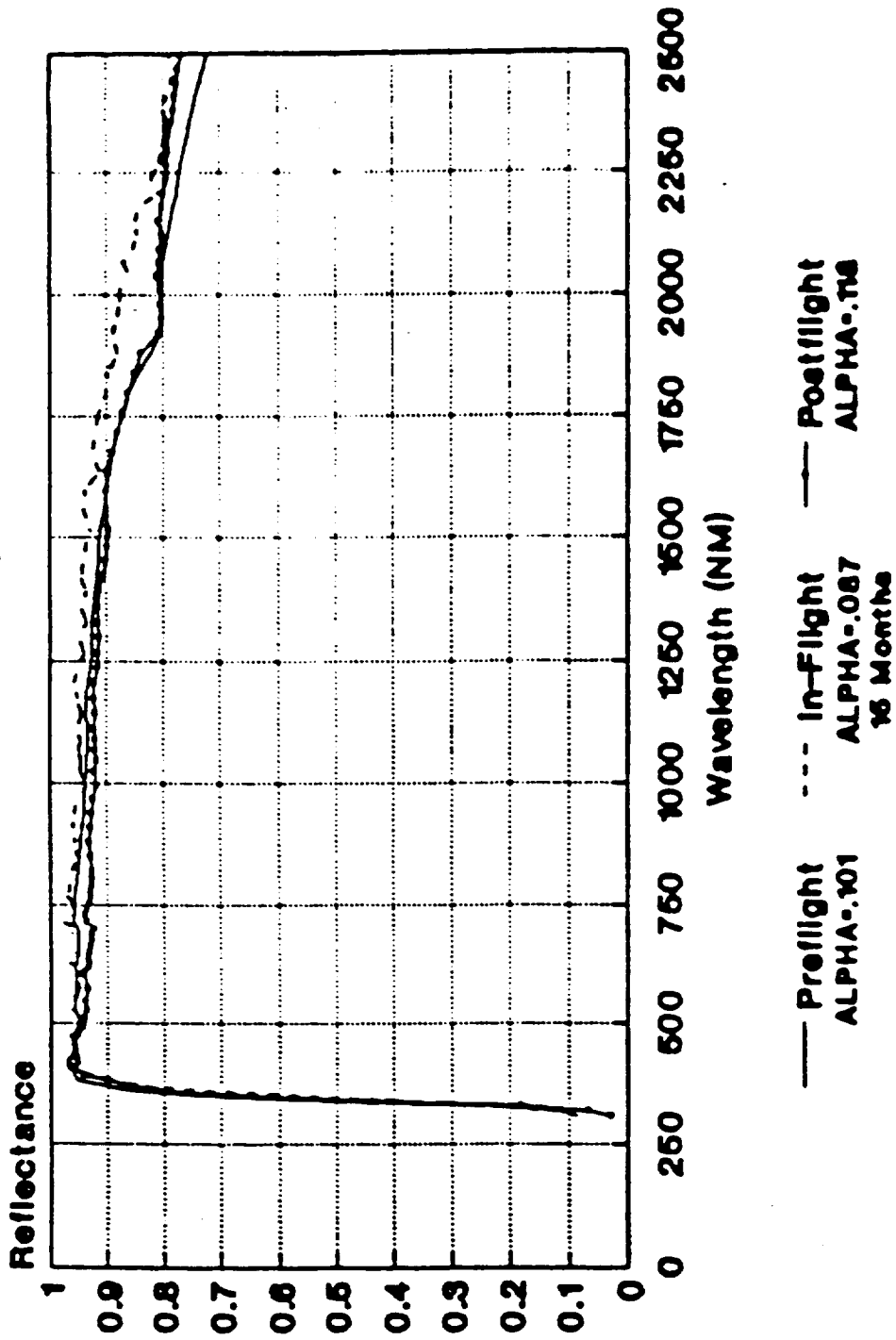


Figure 41. Diffuse solar reflectance for YB71 white thermal control paint.

absorptance. Post-flight analysis indicated that the brown discoloration was attributed to the application of an adhesive which cracked the silver layer and allowed the adhesive to through the cracks and be degraded by the Solar UV. However, only a small change in solar absorptance was measured over the first 16 months of exposure, an indication that the degradation occurred slowly over long space exposure.

#### **4.2.7 Chromic Acid Anodized Aluminum**

One sample of chromic acid anodized aluminum indicated significant degradation during the first 18 months of the mission. When the TCSE batteries were depleted at 19.5 months one sample was left exposed to the environment and the other was protected. These two samples had noticeably different appearance. The sample exposed for 19.5 months had an evenly colored appearance, except for several small surface imperfections. The sample exposed for 69.2 months was mottled and washed out in appearance. Both samples were significantly contaminated with a silica/silicate contaminant. Specimens in an adjacent tray that were anodized in the same batch as the TCSE specimens indicated only a 0.02 change in solar absorptance.

#### **4.2.8 D111 Black**

The D111 diffuse black ceramic samples performed very well, with little change in either visual appearance or optical properties during the LDEF mission. D111 is a non-specular coating made of a carbonaceous pigment in a glass binder. Apparently, the glass binder adequately protects the pigment from AO attack. The flight results are presented in Table 17.

#### **4.2.9 Z302 Black Paint**

Z302 is a glossy black thermal control paint made from carbon black pigments in a polyurethane binder. Z302 is known to be susceptible to AO attack and several samples were flown with protective overcoats of either OI650 or RTV670. Two unprotected samples, which were exposed for the entire mission, eroded down to the primer coat. Two other samples, which were exposed for only 19.5 months, eroded but still had good reflectance properties. As with the A276 overcoats, the overcoated Z302 was observed to contain cracks and peels during post-flight analysis but showed little change in solar absorptance.

#### **4.2.10 Z306 Black Paint**

Chemglaze Z306 is a flat black thermal control paint made from titanium dioxide and carbon in a polyurethane binder. Z306 was the primary thermal control coating on all LDEF interior structural members and experiment tray bottoms. The Z306 on the interior surfaces, which were not subjected to AO or UV, showed good durability. On exterior surfaces and the leading edge tray clamps the Z306 was almost completely eroded away from the composite substrate to which it was applied. The red coloration characteristic of the primer pigment was visible and significant erosion into the composite substrate was observed. Based on the coating thickness, the erosion rate of Z306 is estimated to be at least  $5 \times 10^{-25} \text{ cm}^3/\text{O atom}$ .

#### 4.2.11 Conclusions

Continuous monitoring of solar absorptance for the LDEF materials was not possible because: i) most experiments were passive, returning no data in flight, and ii) the LDEF batteries expired after about 1.5 years, leaving the majority of the mission without a means to capture data on the spacecraft. Because the LDEF saw most of its AO fluence late in the mission recovery effects due to AO may have altered some of the degrading effects of the Solar UV. Nevertheless, some significant conclusions can be made about the LDEF findings.

- White thermal control paints Z93 and YB71 are stable, while A276 is degraded by both AO and UV radiation. Potassium silicate binders are stable, while organic binders are not
- D111 black thermal control paint is stable.
- Chromic acid anodized aluminum is stable.
- UV accelerates AO erosion of Teflon and FEP erodes more rapidly than predicted. The silver Teflon blankets were eroded by AO, but remained functional. On LDEF only 0.001 inches was eroded from the original 0.05 inch film. For longer lifetimes or higher AO fluences the functionality of silver Teflon blankets may be a concern.
- Surface crazing was found in clear silicone coatings, reducing their usefulness as AO protective overcoats.

#### 5 SUMMARY

Several significant comparisons can be made as the result of this study. They are grouped into the areas of space environment models, materials chemistry, and materials exposure results.

There appear to be significant differences in the US and Russian space environment measurements and models. Specifically, the Russian measurements of F10.7 exceed the US values by 25% during solar maximum despite showing good agreement during solar minimum. Similarly, the neutral atmospheric density predicted by Russian models exceeds the corresponding US value by a factor of 3 - 10, with the greater difference occurring at higher altitudes, (1000 km). Finally, the Russian radiation models appear to predict a slightly greater radiation environment in comparison to US models. Consequently, for the same spacecraft orbit the Russian and US models would predict significantly different environmental exposure conditions. This makes comparison of flight test results difficult and also complicates cooperation on future space missions as, pending resolution of these differences, US and Russian designers would deduce different requirements for the same space vehicle. This is a subject that warrants further investigation.

The most significant overlap in materials chemistry occurs for two types of white thermal control paint and for acid anodized aluminum. Both countries utilize zinc oxide and zinc oxide orthotitanate pigments in metasilicate binders. Russian experience broadens to the use of silicone and acrylic resins and asbestos paper while the US relies more heavily on polyurethane.

Finally, both the LDEF and RCC-1 results confirm that zinc oxide and zinc oxide orthotitanate in metasilicate binders, (Z93, YB71, TP-co-2, TP-co-11, TP-co-12) are the most stable upon exposure to the space environment.

This makes these materials leading candidates for use on future, international space ventures such as the Space Station. The solar absorptance and emittance values for these materials are very similar, indicating consistency of results. Even the diffuse reflectance spectra for TP-co-2 and TP-co-12 are in general agreement with the US equivalent Z93. The same is true for TP-co-11 and YB71.

In conclusion, the RCC-1 experiment confirms some of the more significant TCC findings made by the LDEF, minimizing the potential for materials incompatibility on future flights. However, the analysis techniques point to significant differences in space environment model development, making this a key area for further study. While these results presented here are significant for the LEO environment other orbits will require additional evaluation. High inclination and geosynchronous orbits will have the added effects of charged particle radiation, and a possible absence of AO. The synergism between the many effects of Earth orbits requires continued attention.

#### REFERENCES

- <sup>1</sup>Clark, L. G., Kinard, W. H., Carter, D. J., Jr., and Jones, J. L., Jr., (Eds), *The Long Duration Exposure Facility (LDEF): Mission 1 Experiments*, NASA SP-473, 1984.
- <sup>2</sup>LDEF - 69 Months in Space: *First Post-Retrieval Symposium*, NASA CP-3134, 1991.
- <sup>3</sup>LDEF - 69 Months in Space: *Second Post-Retrieval Symposium*, NASA CP-3144, 1992.
- <sup>4</sup>LDEF - 69 Months in Space: *Third Post-Retrieval Symposium*, NASA CP-3275, 1995.
- <sup>5</sup>Hedin, A. E., "MSIS-86 Thermospheric Model," *J. Geophys. Res.*, Vol. 92, No. A5, pp. 4649-4662, (May 1987).
- <sup>6</sup>Linton, R. C., Kamenetzky, R. R., Reynolds, J. M., and Burris, C. L., "LDEF Experiment A0034: Atomic Oxygen Stimulated Outgassing," in *LDEF - 69 Months in Space: First Post-Retrieval Symposium*, NASA CP-3134, p 763, 1991.
- <sup>7</sup>Hemminger, C. S., and Stuckey, W. K., "Space Environmental Effects on Silvered Teflon Thermal Control Surfaces," in *LDEF - 69 Months in Space: First Post-Retrieval Symposium*, NASA CP-3134, p 831, 1991.
- <sup>8</sup>Wilkes, D. R., Brown, M. J., and Zwiener, J. M., "Initial Materials Evaluation of the Thermal Control Surfaces Experiment (S0069)," in *LDEF - 69 Months in Space: First Post-Retrieval Symposium*, NASA CP-3134, p 899, 1991.

- <sup>9</sup>Sampair, T. R., and Berrios, W. M., "Effects of Low Earth Orbit Environment on the Long Duration Exposure Facility Thermal Control Coatings," in *LDEF - 69 Months in Space: First Post-Retrieval Symposium*, NASA CP-3134, p 935, 1991.
- <sup>10</sup>Golden, J. L., "Results of Examination of the A276 White and Z306 Black Thermal Control Paint Disks Flown on LDEF," in *LDEF - 69 Months in Space: First Post-Retrieval Symposium*, NASA CP-3134, p 975, 1991.
- <sup>11</sup>Stein, B. A., "LDEF Materials Overview," in *LDEF - 69 Months in Space: Second Post-Retrieval Symposium*, NASA CP-3144, p. 741, 1992.
- <sup>12</sup>Wilkes, D. R., Miller, E. R., Zwiener, J. M., and Mell, R. J., "The Continuing Materials Analysis of the Thermal Control Surfaces Experiment (S0069)," in *LDEF - 69 Months in Space: Second Post-Retrieval Symposium*, NASA CP-3144, p. 1061, 1992.
- <sup>13</sup>Golden, J. L., "Selected Results for LDEF Thermal Control Coatings," in *LDEF - 69 Months in Space: Second Post-Retrieval Symposium*, NASA CP-3144, p. 1099, 1992.

REPORT DOCUMENTATION PAGE			Form Approved OMB No. 0704-0188	
Public reporting burden for this collection of information is estimated to average 1 hour per response, including the time for reviewing instructions, searching existing data sources, gathering and maintaining the data needed, and completing and reviewing the collection of information. Send comments regarding this burden estimate or any other aspect of this collection of information, including suggestions for reducing this burden, to Washington Headquarters Services, Directorate for Information Operations and Reports, 1215 Jefferson Davis Highway, Suite 1204, Arlington, VA 22202-4302, and to the Office of Management and Budget, Paperwork Reduction Project (0704-0188), Washington, DC 20503.				
1. AGENCY USE ONLY (Leave blank)	2. REPORT DATE March 1995	3. REPORT TYPE AND DATES COVERED Contractor Report (11/8/93-8/12/93)		
4. TITLE AND SUBTITLE Low Earth Orbit Thermal Control Coatings Exposure Flight Tests: A Comparison of U.S. and Russian Results			5. FUNDING NUMBERS C NAS1-19243, Task 16 WU 233-03-02-02	
6. AUTHOR(S) A. C. Tribble, R. Lukins, E. Watts, S. F. Naumov, V. K. Sergeev				
7. PERFORMING ORGANIZATION NAME(S) AND ADDRESS(ES) Rockwell International Space Systems Division Downey, CA 90241			8. PERFORMING ORGANIZATION REPORT NUMBER	
9. SPONSORING / MONITORING AGENCY NAME(S) AND ADDRESS(ES) National Aeronautics and Space Administration Langley Research Center Hampton, VA 23681-0001			10. SPONSORING / MONITORING AGENCY REPORT NUMBER NASA CR-4647	
11. SUPPLEMENTARY NOTES Langley Technical Monitor: Joan G. Funk				
12a. DISTRIBUTION / AVAILABILITY STATEMENT Unclassified-Unlimited Subject Category 23			12b. DISTRIBUTION CODE	
13. ABSTRACT (Maximum 200 words) Both the United States (US) and Russia have conducted a variety of space environment effects on materials (SEEM) flight experiments in recent years. A prime US example was the Long Duration Exposure Facility (LDEF), which spent 5 years and 9 months in low Earth orbit (LEO) from April 1984 to January 1990. A key Russian experiment was the Removable Cassette Container experiment, (RCC-1), flown on the Mir Orbital Station from 11 January 1990 to 26 April 1991. This paper evaluates the thermal control coating materials data generated by these two missions by comparing: environmental exposure conditions, functionality and chemistry of thermal control coating materials, and pre- and post-flight analysis of absorptance, emittance, and mass loss due to atomic oxygen erosion. It will be seen that there are noticeable differences in the US and Russian space environment measurements and models, which complicates comparisons of environments. The results of both flight experiments confirm that zinc oxide and zinc oxide orthotitanate white thermal control paints in metasilicate binders, (Z93, YB71, TP-co-2, TP-co-11, and TP-co-12), are the most stable upon exposure to the space environment. It is also seen that Russian flight materials experience broadens to the use of silicone and acrylic resin binders while the US relies more heavily on polyurethane.				
14. SUBJECT TERMS Thermal control coatings, low Earth orbit, flight data			15. NUMBER OF PAGES 64	
			16. PRICE CODE A04	
17. SECURITY CLASSIFICATION OF REPORT Unclassified	18. SECURITY CLASSIFICATION OF THIS PAGE Unclassified	19. SECURITY CLASSIFICATION OF ABSTRACT Unclassified	20. LIMITATION OF ABSTRACT UL	